Effects of anode materials on electricity production from xylose and treatability of TMP wastewater in an up-flow microbial fuel cell

Johanna Haavisto [a,#], Paolo Dessì [a, b, #,], Pritha Chatterjee [a,c], Mari Honkanen [d], Md Tabish Noori [e], Marika Kokko [a], Aino-Maija Lakaniemi [a], Piet N. L. Lens [a, b], Jaakko A. Puhakka [a]*

[a]*Tampere University, Faculty of Engineering and Natural Sciences, PO Box 541, FI-33104 Tampere University, Finland*

[b]*National University of Ireland Galway, Microbiology, School of Natural Sciences and Ryan Institute, University Road, Galway, H91 TK33, Ireland*

[c]*Indian Institute of Technology Hyderabad, Department of Civil Engineering, Hyderabad, India*

[d]*Tampere University, Tampere Microscopy Center, PO Box 692, FI-33104 Tampere University, Finland*

[e]*Kyung Hee University, Department of Environmental Science and Engineering, 446701 Seoul, South Korea*

Manuscript submitted to: Chemical Engineering Journal

*****Corresponding author: Phone: +353 830678774, e-mail: paolo.dessi@nuigalway.ie, mail: National University of Ireland Galway, Microbiology, School of Natural Sciences and Ryan Institute, University Road, Galway, H91 TK33, Ireland

[#] These two authors contributed equally to the manuscript

List of abbreviations

AEM, anion exchange membrane

APHA, animal and plant health association

CE (%), coulombic efficiency

CEM, cation exchange membrane

COD (g/L), chemical oxygen demand

CV, cyclic voltammetry

EDTA, ethylenediaminetetraacetic acid

EIS, electrochemical impedance spectroscopy

GAC, granular activated carbon

GC-FID, gas chromatograph-flame ionization detector

HPLC, high performance liquid chromatography

HRT (days), hydraulic retention time

LSV, linear sweep voltammetry

MFC, microbial fuel cell

OCV (V), open circuit voltage

R_{ct}, charge transfer resistance

RID, refractive index detector

R_s, ohmic resistance

SEM-EDS, scanning electron macroscope-energy dispersive x-ray spectroscopy

SS, stainless steel

TMP, thermomechanical pulping

TS (g/L), total solids

TSS (g/L), total suspended solids

VFA (g/L), volatile fatty acid

VS (g/L), volatile solids

VSS (g/L), volatile suspended solids

Abstract

The aim of this study was to determine an optimal anode material for electricity production and COD removal from xylose containing synthetic wastewater in an up-flow microbial fuel cell (MFC), and assess its suitability for treatment of thermomechanical pulping (TMP) wastewater with an enrichment culture at 37 °C. The anode materials tested included carbon-based electrodes (graphite plate, carbon cloth and zeolite coated carbon cloth), metal-based electrodes (tin coated copper) and a metal-carbon assembly (granular activated carbon in stainless steel cage). During continuous operation with xylose COD removal was 77-86% of which 25-28% was recovered as electricity. The highest power density of 333 (± 15) mW/m^2 was obtained with the carbon cloth electrode. However, based on an overall analysis including electrode performance, surface area and scalability, the granular activated carbon in stainless steel cage (GAC in SS cage) was chosen to be used as electrode for bioelectrochemical treatment of TMP wastewater. The TMP fed MFC was operated in continuous mode with 1.8 days hydraulic retention time, resulting in 47 (± 13%) COD removal of which 1.7% was recovered as electicity with the average power production of 10-15 mW/m^2. During operation with TMP wastewater, membrane fouling increased the polarization resistance causing a 50% decrease in power production within 30 days. This study shows that MFC pretreatment removes half of the TMP wastewater COD load, reducing the energy required for aerobic treatment.

Keywords: Electricity production, Electrode material, Granular activated carbon, Membrane fouling, Microbial electrochemical technology, Thermomechanical pulping wastewater

1. Introduction

Pulp and paper mills generate 10-100 m^3 of wastewater per ton of produced paper [1]. Such wastewaters may contain hundreds of organic and inorganic compounds, depending on the process where they are generated, and could therefore pollute the receiving water bodies if released untreated [2]. The cost associated with aerobic treatment of pulp and paper wastewaters, characterized by an organic load of 1-10 g/L chemical oxygen demand (COD) [1] is pushing towards implementation of an anaerobic treatment. This would result in energy recovery, e.g. in the form of biogas or bioelectricity, as well as decreasing the cost of the successive aerobic treatment step [3].

Thermomechanical pulping (TMP) wastewater is a potential substrate for anaerobic bioprocesses, as it is rich in carbohydrates (25-40 % of the total COD) [3]. In addition, TMP wastewater contains only small concentrations of inhibitory compounds, such as fatty acids, resin acids, hydrogen peroxide, sulphite, and sulphate, which are more typical in chemical pulping wastewater [1]. Biological energy production from TMP wastewater has been demonstrated in the form of methane [4,5] and hydrogen [6].

Direct conversion of organic compounds into electricity in microbial fuel cells (MFCs) is a promising alternative for harnessing energy from wastewaters [7,8]. In MFCs, an anodic

biological reaction is combined to a cathodic biotic or abiotic reaction to harness electrical energy from organic and inorganic substrates [9]. A variety of wastewaters has been used for electricity production in MFCs, including municipal [10,11], agricultural [12], and industrial wastewaters [13–15]. Despite its relatively high concentration of readily degradable carbohydrates and acetic acid [3], TMP wastewater has not yet been investigated for bioelectricity production and COD removal in MFCs.

The adoption of MFCs for wastewater treatment in large scale is currently hindered by the high cost of the materials, particularly the electrodes and membranes, and the low power densities [7]. In MFCs, an efficient anode electrode should be biocompatible, conductive, resistant to corrosion, and have a high surface area [16]. Carbon-based electrode materials are less conductive than metal-based materials, but are usually of lower-cost, more biocompatible and have a higher surface area [17]. Graphite plate and carbon cloth are widely studied carbon based anode materials, from which conductive carbon cloth with high surface area has shown its potential in many studies [17]. It has also been suggested that multi-material electrodes, e.g. combinations of carbon and metal materials, can significantly increase power production compared to plain carbon or metal electrodes [18,19]. Addition of functional groups to the anodic surface, for example, pretreating the electrode with ammonium or acids, facilitates electron transfer and bacterial attachment [20,21]. Hydrophilic zeolite coating has also been tested to increase bacterial attachment by enabling access of polar sugar molecules, which attract bacteria on the electrode surface [22]. In addition, the electrodes should have a large surface area and be easily scalable. An example of such material is granular activated carbon (GAC). Granular anode materials are exploited, e.g. in fluidized bed MFCs where moving particles

collide with a current collector [23] or trapped in a conductive metal cage. In both cases, GAC offers a large surface area for microbial adhesion and charge accumulation. Furthermore, the capacitive nature of GAC enables charge transfer when fluidized or loosely packed granules are in contact with current collectors [24]. MFCs with capacitive anode materials can also be operated by repeating open and closed circuit cycles to increase the power density [25].

The purpose of this study was to compare carbon-based (graphite plate and carbon cloth, with and without zeolite coating), metal-based (tin coated copper) and metal-carbon composed (GAC in stainless steel cage) anode electrode materials for electricity production and COD removal in a continuous xylose-fed up-flow MFC with a mixed culture. The most promising anode material was then utilized to assess the bioelectrochemical treatment of TMP wastewater in MFCs in terms of electricity generation and COD removal.

2. Materials and methods

2.1 Inoculum and synthetic wastewater

The up-flow MFC used in this study was inoculated with effluent from another xylose fed up-flow MFC operated at 37 °C originally inoculated with anaerobic sludge (same seed as described by Haavisto et al. [26]) from a municipal wastewater treatment plant. The synthetic wastewater was prepared as described by Mäkinen et al. [27] without addition of EDTA and resazurin. The concentration of yeast extract was 0.02 g/L at start-up, and was omitted during continuous feeding. Xylose (1.0 g/L) was used as the substrate, and pH of the medium was adjusted to 7.0 with NaOH. The conductivity of the medium was 12-13 mS/cm.

2.2 Thermomechanical pulping wastewater

The wastewater used in this study, collected from a pulp and paper mill in Finland, was effluent of a thermomechanical pulping (TMP) process, in which wood was steamed at approximately 120 °C to obtain the pulp. The TMP wastewater had a pH of 5.1 and a composition as specified in Table 1. To minimize changes in the composition upon storage, which was demonstrated in a previous study [6], the TMP wastewater was kept at -20 °C in either 2 L or 5 L containers, and defrosted 24 hours before use. To keep the pH close to 7.0 and increase the buffering capacity, $NaHCO_3$ (0.8 or 2 g/L, as specified in section 2.5) was added to the TMP wastewater. The conductivity of the TMP wastewater was 1.4 mS/cm and increased to 2.0 and 2.9 mS/cm after adding 0.8 and 2 g/L $NaHCO_3$, respectively. After defrosting and addition of $NaHCO_3$, the TMP wastewater was settled in a 2 L container for 12 hours at 4 °C prior to utilization. The supernatant was then flushed with N_2 for 5 min prior to being fed to the up-flow MFC.

Table 1. Characteristics of the thermomechanical pulping (TMP) wastewater.

Parameter	**Concentration (mg/L)**
TS	4415 ± 30
VS	3350 ± 125
TSS	807 ± 148

VSS	755 ± 143
Total COD	3512 ± 77
Soluble COD	3170 ± 16
Total nitrogen	7.6 ± 0.2
Phospate phosphorous (PO_4^{3-}-P)	2.4 ± 0.1
Total dissolved saccharides	1112 ± 190
Acetate	279 ± 10
Alkalinity[a]	114 ± 1
Sodium	162.0 ± 0.0
Potassium	22.8 ± 0.2
Magnesium	4.2 ± 0.0
Calcium	43.9 ± 0.1

[a] Measured as mg HCO_3^-/L

2.3 Anode electrodes

The anode electrodes used for comparison were: i) graphite plate, ii) carbon cloth, iii) carbon cloth with zeolite coating, iv) tin coated copper mesh, and v) granular activated carbon in stainless steel cage (GAC in SS cage) (Fig. S1). All electrodes used for comparison had a projected surface area (including both sides of the electrode) of 0.0056 m^2, whereas the GAC in SS cage electrode used for TMP wastewater treatment was up-scaled to 0.0080 m^2. The graphite plate, carbon cloth (with and without zeolite) and tin coated copper electrodes were connected to a copper wire with conductive silver glue, which was covered with epoxy after hardening to prevent oxidation.The steel cage electrodes were sewed with Ti wire and the long end of the wire was used as electric wire (Fig. S1).

The graphite plate electrode was prepared by drilling holes on a graphite plate (McMaster-Carr, Aurora, OH) and reinforcing the electrical wire connection with a screw. The electrode was stored for two days in 1 M NaOH and rinsed with MilliQ® water prior to utilization. The graphite plate surface contained irregular surface structures with shapes <10 µm in size according to scanning electron microscope (SEM) images (Fig. S2).

The carbon cloth electrodes had a fiber diameter of approximately 10 µm (Fig. S2) and the edges were reinforced with superglue to prevent fraying. Zeolite coating was done using sodium silicate and sodium aluminate solutions as described by Balkus and Ly [28]. Prior to coating, the electrode was pretreated in 10% HNO_3 solution at 90 °C for 3 hours to increase the NaX zeolite attachment by introducing N-groups on carbon and making the carbon more hydrophilic [29]. Sodium silicate, sodium aluminate solutions and MilliQ® water were mixed after cooling down to room temperature until a homogenous mixture was formed and the electrode was immersed in the mixture immediately. The mixture was then treated at 90 °C for 3 hours in a plastic container followed by rinsing with MilliQ® water. The presence of zeolite crystals on the electrode was confirmed by SEM-energy dispersive x-ray spectroscopy (EDS) analysis. Small crystals (<1 µm in size, Fig. S2) contained Na, Si, O, and Al, which are the elements belonging to NaX zeolite [22].

The tin coated copper mesh anode electrode consisted of two overlapping mesh sheets (Canopy mesh fabric, Cat. #1208, Less EMF Inc.). The edges were treated with epoxy to prevent oxidation. The surface of the tin coated wire was smooth as shown by the SEM images (Fig. S2).

The GAC in SS cage anode electrode was prepared by pouring 9.2 g (for electrode comparison) or 15 g (for TMP wastewater treatment) of granular activated carbon (< 2 mm, Alfa Aesar) into a tightly folded stainless steel sheet (Tilox, 30 wires per inch, wire thickness 0.165 mm) sewed with Ti wire. The electrode was immersed in water overnight before use. Based on SEM, the granules had a very rough surface with irregularities varying from <1 µm to >1 mm (Fig. S2).

2.3 Up-flow MFC set-up

The up-flow MFC, described by Lay et al. [30] , consisted of a 500 mL anodic chamber and a 250 mL cathodic chamber separated by an anion exchange membrane (AEM) AMI-7001 or a cation exchange membrane (CEM) CMI-6001 (Membranes International Inc., USA), as specified in section 2.4. Both membranes had a diameter of 4.5 cm. The catholyte was 250 mL of potassium ferricyanide (50 mM) in phosphate buffer (100 mM Na_2HPO_4, pH 7.0). Anode and cathode electrodes were connected through a 100 Ω resistor. A reference electrode (Ag/AgCl SENTEK QM710X in 3 M KCl) was connected to the recirculation tube through a glass capillary (QiS, the Netherlands). The temperature of the anode chamber was kept stable at 37 (± 1) °C using heating coils. The anolyte was recirculated at a flow rate of 60 mL/min using a peristaltic pump (Masterflex, USA). The cathode electrode was a graphite plate (0.00385 m^2, McMaster-Carr, Aurora, OH) pretreated for one hour with 1 M HCl, stored overnight in NaOH and rinsed with MilliQ® water prior to use. Sampling ports were located in the anode chamber inlet and outlet tubes.

2.4 Up-flow MFC operation

For electrode comparison, the up-flow MFC was started with 450 mL of xylose-containing synthetic wastewater and 50 mL of inoculum. The MFC was operated semi-continuously with each electrode until a similar power density (<10% difference in maximum power densities) was obtained in three consecutive feeding cycles (5-7 days/cycle), and then switched to continuous mode (3.5 days HRT). To avoid depletion of the electron acceptor during continuous feeding, the catholyte was changed 2-3 times per week.

Prior to operation with TMP wastewater, the MFC was started up with the xylose-containing synthetic wastewater (450 mL), without inoculum, for 24 hours, resulting in a voltage output of < 3 mV. Then, 50 mL of inoculum, previously stored at 4 °C for 7 days, was added and the MFC was operated in continuous mode for 22 days with 1 day HRT to reactivate the microbial community after storing. On day 23, the synthetic wastewater was replaced with thermomechanical pulping (TMP) wastewater, supplemented with 0.8 g/L $NaHCO_3$ (Fig. 1). The MFC was then operated in semi-continuous mode with TMP wastewater for two cycles of approximately 6 days each. On day 35, the MFC was switched to continuous mode. The HRT was set to 1.8 days due to the higher COD concentration (Table 1) and substrate recalcitrance of the TMP wastewater compared to the synthetic wastewater. On day 39, the $NaHCO_3$ concentration was increased to 2 g/L to keep the pH close to 7. On day 45, the AEM was replaced with a CEM and the MFC was operated with a CEM until day 178 (Fig. 1). Between days 1-108, the membrane was replaced periodically (approximately once per month) with a new one when the performance of the MFC was not restored after changing the catholyte. When changing the membrane, the catholyte solution was completely replaced (250 mL) with fresh ferricyanide solution. Between days 108-178, the CEM was not changed anymore in order to see how the prolonged operation with the same CEM affects the power production and effluent quality.

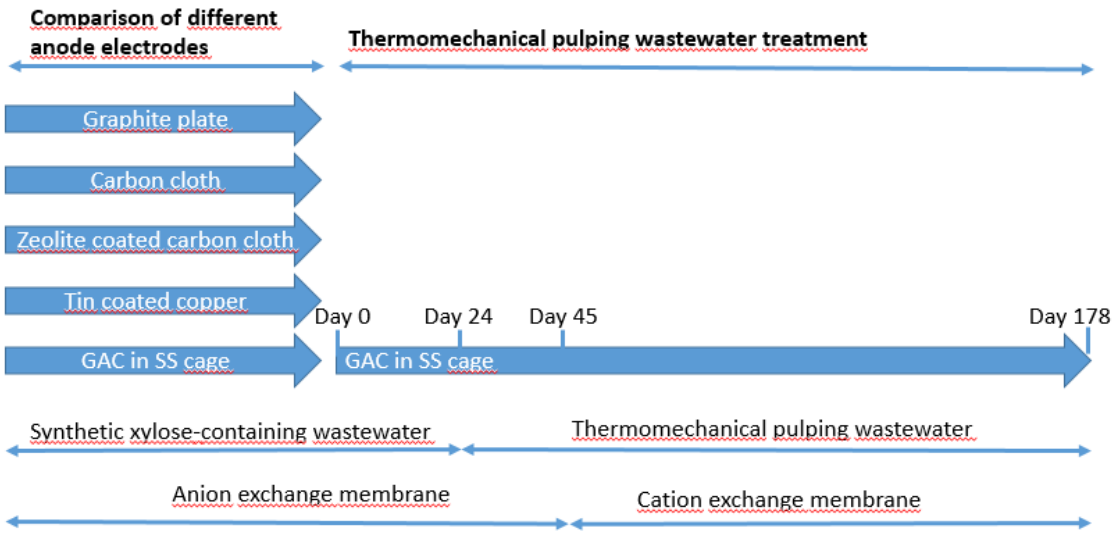

Fig. 1. Flow chart of the MFC studies presenting anode electrode comparison (26-42 days) and thermochemical wastewater treatment (178 days). Synthetic xylose-containing wastewater was used in the anode electrode comparison and for the start-up of thermomechanical pulping (TMP) wastewater treatment until the feeding solution was changed to TMP wastewater on day 24. An anion exchange membrane was used during the anode electrode comparison and changed to cation exchange membrane during TMP wastewater treatment (on day 45).

2.5 Analytical methods

During semi-continuous operation, anolyte samples were collected after every feeding, whereas during continuous feeding the anolyte inlet and outlet samples were collected every 2-3 days. The total and soluble COD was measured using the dichromate method according to the Finnish standard SFS 5504. Conductivity and pH were measured with a conductivity meter (Horiba LAQUAtwin, Japan) and a pH meter (WTW pH 330 meter with Hamilton Slimtrode probe), respectively. Alkalinity, total solids, volatile solids, total suspended solids and volatile suspended solids were measured according to the APHA standards [31]. Cations were measured using DX-120 ion chromatograph (Dionex, USA) with AS40 autosampler, IonPac CS12A cation exchange

column and CSRS 300 suppressor (4 mm). The eluent contained 2 mM methane sulphonic acid and the flow rate was 1 mL/min. Total nitrogen and phosphate phosphorous (PO_4^{3-}-P) were measured using the Hach (USA) Lange kits LCK 238 and LCK 349, respectively, following the supplier's instructions.

Total dissolved saccharides were measured as glucose equivalents by a colorimetric method modified from Dubois et al. [32]. The reactions contained 1 mL sample, 0.5 mL 5% phenol solution, and 2.5 mL sulfuric acid and absorbance was measured at 485 nm wavelength. Monosaccharides (glucose, xylose, arabinose, galactose and cellobiose) were measured by a high performance liquid chromatography (HPLC) system equipped with a Rezex RPM-Monosaccharide Pb^+ column (Phenomenex, USA) held at 85 °C and a refractive index detector (RID). MilliQ® water was used as the mobile phase at a 0.6 mL/min flow rate. Volatile fatty acids (VFAs) and alcohols were measured by a gas chromatograph (Shimadzu Ordior GC-2010 plus) with ZB-WAXplus column (Phenomenex, USA) and a flame ionization detector (GC-FID) as described by Haavisto et al. [33]. For the soluble COD and the VFA analysis, the samples were filtered with 0.45 µm syringe filters, whereas for the monosaccharides analysis with HPLC the samples were filtered with 0.2 µm syringe filters.

The surface of the CEM and the anode electrodes were studied by imaging and elemental analysis with a scanning electron microscope (SEM, ULTRAplus, Zeiss, Germany) equipped with an energy dispersive spectrometer (EDS, INCAx-act silicon-drift detector, Oxford Instruments, United Kingdom). The CEM was considered fouled when power production did not increase after changing the catholyte, approximately after 30 days of continuous up-flow MFC

operation with TMP wastewater. Triplicate samples (approximately 1 × 1 cm) were cut from a fouled membrane by sterile scissors on day 101. A sample of unused CEM was also collected as a negative control. The samples were fixed in 4% paraformaldehyde and dehydrated with increasing ethanol concentration (25, 50, 75, 90 and 100%). Both electrode and membrane samples were attached on aluminium SEM stubs. Membrane samples were further coated with carbon to avoid sample charging during SEM-EDS analysis.

2.6 Electrochemical analyses

Voltage and anode potential (reported *vs.* Ag/AgCl reference electrode) were measured at a two minute interval using a data logger (Agilent 34970A, Agilent technologies, Canada). When comparing the anode electrodes, linear sweep voltammetry (LSV) and cyclic voltammetry (CV) were done with 0.001 V steps and 0.001 V/s scan rate, respectively, using a potentiostat (Palmsens3, Netherlands) after at least 10 days operation in continuous mode. For the GAC in SS cage electrode, CV analysis was repeated with another measurement device (BioLogic VMP3, France) as the current density (> 5.4 A/m^2) exceeded the upper detection limit of the Palmsens potentiostat. Both LSV and CV were performed after 30 min of stabilization in open circuit mode and the catholyte solution was changed before the measurements. The whole cell LSV limit was set to 0-50 mV above the open circuit voltage (OCV), whereas anodic CV and LSV were recorded between the anode potentials of -0.525 V and +0.2 V *vs.* Ag/AgCl.

During MFC operation with TMP wastewater, power and polarization curves were obtained on day 82 (with fresh CEM) and on day 94 (with fouled CEM) as previously described by Dessì et al. [34]. Whole cell electrochemical impedance spectroscopy (EIS) was performed on day 99

(with fouled CEM) and on day 105 (with fresh CEM) using a potentiostat (BioLogic VMP3, France) in a three-electrode set-up. The AC amplitude was set to 10 mV and the frequency was varied from 1 MHz to 0.1 Hz with 6 steps per decade. The EIS spectra were simulated in EC-Lab V11.21 software (BioLogic VMP3, France) using a best fit circuit to obtain different impedance values. The randomised simplex method with 5000 iteration was used for fitting and simulation.

2.7 Calculations

Current and power densities were calculated according to Ohm's law [9] and normalized to the projected anode surface area (0.0056 m^2 for electrode comparison or 0.0080 m^2 for TMP wastewater treatment) or anode chamber volume (500 mL). Average stable current and power densities for electrode comparison were calculated during three separate stable 24 h periods after catholyte replacements when current densities did not vary more than 3% (later referred to as current and power densities). The internal resistance was estimated either from the LSV data, or from the slope of the polarization curve [9]. During anode material comparison, theoretical COD and electrons in the influent and effluent were calculated according to Van Haandel and Van der Lubbe [35] by converting xylose and VFA concentrations from the stable operation period to COD equivalents. Coulombic efficiency (CE) was calculated according to Logan et al. [9] based on theoretical COD removal (determined by calculating xylose and VFAs as COD equivalents) during electrode comparison, or on the total COD removal when the MFC was operated with TMP wastewater.

3. Results and discussion

3.1 Bioelectrochemical treatment of xylose-containing synthetic wastewater with different anode materials

3.1.1 Power and current production

Power densities between 265 and 333 mW/m^2 were obtained from xylose in a continuous MFC operation with the different carbon-based anode materials (Table 2). A slightly higher one-day average power density of 358 mW/m^2 was obtained with the tin coated copper mesh electrode on day 2 of semi-continuous operation. However, the power density declined on day 3 (Fig. S3) due to copper oxidation and solubilization. Copper has an excellent electrical conductivity and is widely used in electrical wires, but it is not stable in oxidative environments, such as the anodic chamber, and forms copper oxides toxic to microorganisms [36]. The results of Zhu and Logan [36] also indicated that copper corrosion can result in abiotic current production in MFCs. Despite the tin coating used in this study to prevent corrosion [37], the dark color of the electrode (Fig. S1) suggested its oxidation during MFC operation. Thus, MFC operation with this electrode was not continued.

A power density of 333 mW/m^2 was obtained with the carbon cloth electrode. Zeolite coating on carbon cloth, with pretreatment in 10% HNO_3 solution, decreased the power density by 20% in this study, which is in disagreement to Wu et al. [22], who reported a 152% increase in power density after applying a zeolite coating on a graphite felt. In this study, zeolite coated carbon cloth was also studied without the pretreatment in 10% HNO_3 solution, but due to the similar power densities (254 ± 10 mW/m^2) and CV curves (results not shown) to the zeolite coated carbon cloth with pretreatment, only the results with pretreatment are compared with the other electrodes. The power density with the graphite plate electrode (309 mW/m^2) was lower

compared to non-coated carbon cloth, as was also reported by Pocaznoi et al. [38].The GAC in SS cage electrode resulted in a power density of 274 mW/m^2 (18% smaller than with the non-coated carbon cloth). The GAC was not fixed on the surface of the stainless steel mesh, and the loose contact of the irregularly shaped porous particles may have caused the relatively high internal resistance [39], which was the second highest (72 Ω) among the electrodes, after the zeolite coated carbon cloth (Table 2).

Table 2. Effect of anode material on production of stable power and current densities, anode potential (mV *vs.* Ag/AgCl), and cell internal resistance according to linear sweep voltammetry obtained with the different electrode materials during continuous feeding.

Anode electrode	Power density (mW/m^2)	Power density (W/m^3)	Current density (A/m^2)	Anode potential (mV)	Internal resistance (Ω)
Carbon cloth	333 ± 15	3.7 ± 0.2	0.77 ± 0.02	-433 ± 2	54
Graphite plate	309 ± 15	3.5 ± 0.2	0.74 ± 0.02	-428 ± 6	61
GAC in SS cage[a]	274 ± 15	3.1 ± 0.2	0.70 ± 0.02	-402 ± 4	72
Zeolite coated carbon cloth	265 ± 14	3.0 ± 0.2	0.69 ± 0.02	-433 ± 2	88

[a] Granular activated carbon in stainless steel cage

Although carbon cloth resulted in the highest current densities during continuous operation (0.77 A/m^2 at an anode potential of -433 mV), turnover CV curves show that at -400 mV anode

potential, the highest current density (1.0 A/m^2) was measured with graphite plate, while the current densities with other materials were 0.24-0.40 A/m^2. Turnover CV curves also show that GAC in SS cage and graphite plate enabled considerabely higher current densities than the other two electrode materials at more positive anode potentials (Fig. 2).

The maximum current densities of bare and zeolite coated carbon cloths were 1.8 and 1.9 A/m^2 at anode potentials of -270 and -300 mV, respectively, but the current densities were suppressed by power overshoot at more positive anode potentials (Fig. 2). Power overshoot is a complex phenomenon and has been suggested to occur due to, e.g., higher electron transfer rate from bacteria to the electrode compared to production rate [40], differences in microbial community composition and the amount of bacterial electron transfer components [41], or limited proton transfer out of the biofilm decreasing the biofilm pH [42]. Both the graphite plate and GAC in SS cage electrode showed higher current densities (>5.2 A/m^2) in the CV analysis compared to carbon cloth at anode potentials higher than -0.19 V. One reason for the high current densities with GAC at a scan rate of 1 mV/s is the capacitance due to the very large surface area, which is a desired property for MFC anodes since it favours both bacterial attachment and charge accumulation [16,23].

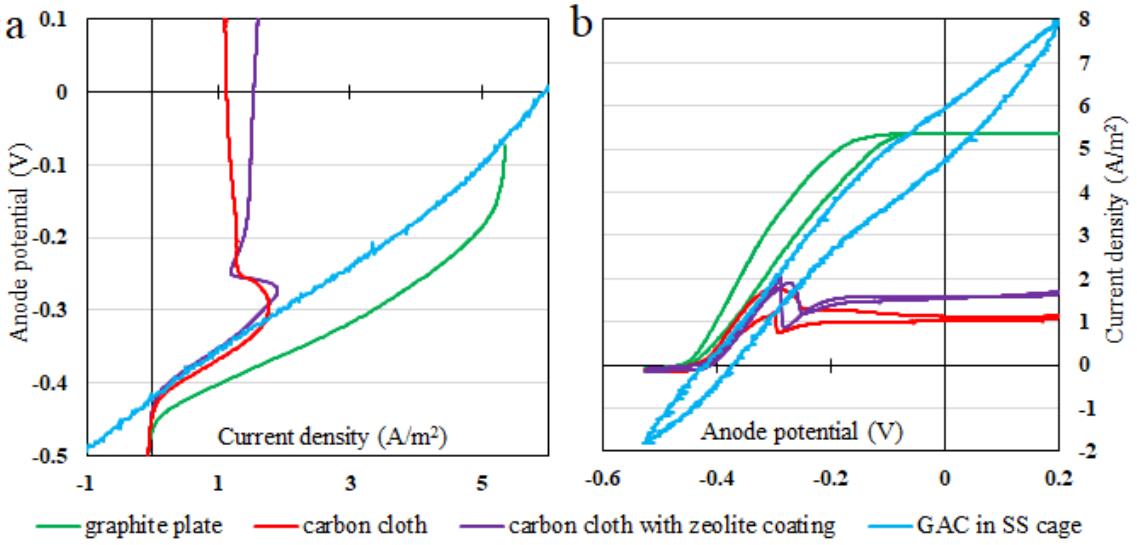

Fig. 2. Anodic linear sweep voltammetry (a) and cyclic voltammetry (b) obtained with the different anode electrodes during continuous MFC operation with xylose. GAC in SS cage stands for granular activated carbon in stainless steel cage.

3.1.2 Treatment of synthetic wastewater

During continuous MFC operation with synthetic wastewater, the xylose removal efficiency was above 95% regardless of the electrode material and the anolyte pH ranged between 6.7 and 7.0. The effluent contained mainly acetate (4-5 mM) and propionate (ca. 1.5 mM). The theoretical COD removal efficiency (calculated from measured VFA and xylose concentrations) was the highest with the carbon cloth (86 ± 1 %) and varied between 77 and 81% with the other electrodes (Table 3). CE varied between 25 and 28%. Electrons in the effluent and current production together accounted for 34-42% of the influent electrons, showing that the majority of the electrons was directed to other processes such as growth and methane generation [43].

Table 3. Theoretical COD removal efficiency (%), share of the supplied electrons (%) in the effluent in the form of acetate, propionate and xylose, and Coulombic efficiency (%) during stable, continuous operation with synthetic wastewater.

Anode electrode	**Theoretical COD removal efficiency (%)**	**Electrons in effluent (%)**	**CE (%)**
Graphite plate	77 ± 4	23 ± 4	28
Carbon cloth	86 ± 1	14 ± 1	26
Zeolite coated carbon cloth	79 ± 9	21 ± 9	25
GAC in SS cage[a]	81 ± 3	19 ± 3	25

[a] Granular activated carbon in stainless steel cage.

3.1.3 Electrode material selection

Electrode selection for bioelectrochemical treatment of TMP wastewater was based on performance criteria (COD removal, power density and obtainable current) and material characteristics (actual surface area and scalability) as summarized in Table 4 (more detailed material scalability comparison is given in Table S1). GAC in SS cage was rated as the best electrode material (Table 4) and selected for TMP wastewater treatment. GAC is an easily scalable electrode material that can be used in various reactor configurations due to its high specific surface area, capacitive behavior and 3D structure [23,24]. Graphite plate and carbon cloth were ranked equally to the second place due to higher COD removal with carbon cloth and higher current density in CV analysis with graphite plate. With zeolite coating on carbon cloth, both the average power density and COD removal efficiency decreased as compared to that of bare carbon cloth. Hence it was ranked fourth. With tin coated copper electrode, the MFCs never

started to generate stable current density due to copper oxidation, hence it was ranked as the least favorable electrode material.

Table 4. Selection criteria for anode electrodes for bioelectrochemical wastewater treatment.

	Performance criteria[a]			**Material characteristics**		
Anode electrode	COD removal[b]	Power density[c]	Current[d]	Actual surface area[e]	Electrode scalability[f]	**Overall rating**
GAC in SS cage	+++	++	++	+++	+++	1.
Carbon cloth	+++	+++	+	+	++	2.
Graphite plate	++	+++	++	+	++	2.
Zeolite coated carbon cloth	++	++	+	+	++	4.
Tin coated	n.a.	n.a.	n.a.	+	+	5.

copper

[a] Based on experimental data of this study

[b] Based on COD removal obtained during continuous feeding (>80% +++ , 60-80% ++, <60% +)

[c] Based on the average, stable power densities under continuous feeding (>300 mW/m^2 +++, 250-300 mW/m^2 ++, <250 mW/m^2 +).

[d] The highest current densities obtained during CV analysis at turnover conditions (>10 A/m^2 +++, 5-10 A/m^2 ++, <5 A/m^2 +).

[e] Surface area of the electrodes calculated for the size of the electrodes used in this study (>1000 m^2 +++, 100-1000 m^2 ++, <100 m^2 +). The specific surface areas are based on literature: carbon cloth Brunauer-Emmett-Teller (BET) 2.39 m^2/g [44]; graphite plate BET 0.6 m^2/cm^2 [45]; GAC 500-2000 m^2/g [46]; tin coated copper mesh area was calculated from electrode weight (1.0 g), copper density (8.96 g/cm^2) and wire diameter (0.1 mm) assuming smooth surface.

[f] Scalability criteria are specified in more detail in Table S1

n.a. Not analysed (current production with tin coated copper deterioted before continuous feeding was started).

3.2 Bioelectrochemical treatment of TMP wastewater

3.2.1 Power production

The up-flow MFC was started with synthetic wastewater containing xylose, at 1 day HRT, obtaining a power of about 150 mW/m^2 (2.4 W/m^3) within the first day of operation (Fig. S4a). However, the power production from xylose gradually decreased with time, being 65 mW/m^2 (1 W/m^3) on day 21, but then increased back to about 150 mW/m^2 after replacing the AEM with a fresh one (Fig. S4a). This suggests that the deterioration of the membrane was decreasing the MFC performance, as previously reported also by Miskan et al. [47].

On day 24, the change of substrate from xylose to TMP wastewater and the change of operation mode from continuous to semi-continuous caused a drop in the power production to as low as 1 mW/m^2 after two feeding cycles (Fig. S4b). The lower power production was likely caused by the lower conductivity of the TMP wastewater compared to the xylose-containing synthetic wastewater (2 mS/cm *vs.* 12-13 mS/cm), which increased the internal resistance and hampered ion transfer [48]. Furthermore, when the MFC was operated in semi-continuous mode, addition of 0.8 g/L $NaHCO_3$ to the TMP wastewater was not enough to prevent acidification of the anolyte. The anolyte pH decreased to below 6 in a few days, likely reducing the activity of anodic microorganisms [49].

Switching the operation mode from semi-continuous to continuous (HRT 1.8 days) on day 35, the power production only slightly increased to 2.5 mW/m^2 (Fig. S4c). After starting the continuous feeding, the pH remained low (< 6). On day 39, increasing the $NaHCO_3$ concentration to 2 g/L not only stabilized the pH to values close to 7 and conductivity to about 3 mS/cm, but also increased the power production to an average of 5 mW/m^2 (Table 5; Fig. S4c). However, it should be noted that the AEM was replaced with a fresh one on day 39 as well, which could have contributed to the increasing power production, especially in the first operating days with the fresh membrane.

On day 45, replacing the AEM with a CEM resulted in a 2 to 3-fold increase in the obtained power density (Table 5). The low power production with the AEM was likely due to the flow of phosphate anions from the cathodic to the anodic chamber [50], which may have caused

precipitation of salts when in contact with the Ca^{2+} ions present in the wastewater (Table 1). Such an issue was mitigated, although not solved, using a CEM (as discussed in section 3.2.3).

Table 5. Average power and current densities, influent and effluent COD, and Coulombic efficiency (CE) obtained in the up-flow MFC continuously fed with thermomechanical pulping wastewater with either an anion or a cation exchange membrane.

Operation days	**Membrane**[a]	**Power density (mW/m^2)**	**Power density (W/m^3)**	**Current density (mA/m^2)**	**Influent COD_{tot}**[b] **(g/L)**	**Effluent COD_{tot}**[b] **(g/L)**	**CE (%)**
39-45	AEM	5.0	0.08	0.08	4.23	3.30	1.7
45-55	CEM	11.0	0.18	0.12	4.94	2.77	1.1
71-91	CEM	15.0	0.24	0.14	4.29	2.38	1.5
108-142	CEM	14.0	0.22	0.13	4.36	1.98	1.1
60-71, 92-101, 147-178	Fouled CEM	2.4	0.04	0.04	4.10	2.00	0.5

[a] AEM, anion exchange membrane; CEM, cation exchange membrane

[b] Total chemical oxygen demand

During the operation in continuous mode (Fig. 3), power peaks of 75-100 mW/m^2 were obtained when the CEM was replaced with a fresh one (on days 45, 71, and 109). This can be attributed to the high surface area of the fresh CEM available for proton exchange, as compared to the used one, in which CEM fouling likely limited proton diffusion (see section 3.2.3). Furthermore, the catholyte was entirely (250 mL) replaced with fresh 50 mM ferricyanide solution when the CEM was changed, increasing the availability of the electron acceptor at the cathode. Within a few days after replacing the CEM, the power decreased to 10-15 mW/m^2 and remained stable for 20-35 days (Fig. 3; Table 5). For longer operation periods, the power production decreased further to an average of 2.4 mW/m^2, and the performance of the MFC was not recovered after replacing the catholyte due to CEM fouling (Fig. 3; Table 5).

An average CE below 2% was obtained from TMP wastewater in the upflow MFC. The CE was calculated based on the total COD removal (i.e. the difference between influent and effluent COD). Although the TMP wastewater was settled before feeding to the MFC, some suspended solids were present in the influent, and accumulated in the MFC. The presence of VFAs in the effluent, as shown in section 3.2.2, suggests that the HRT of 1.8 days was likely not enough for achieve a full conversion of VFAs to electricity, requiring optimization. Electrons may also have been consumed via reduction of sulphate, found in TMP wastewater with concentrations of 140-300 mg/L [5], whereas methane or hydrogen were not detected in the gas bag. A small share of electrons was likely directed to microbial growth, or stored as polymers in the microorganisms due to the abundance of external carbon [51].

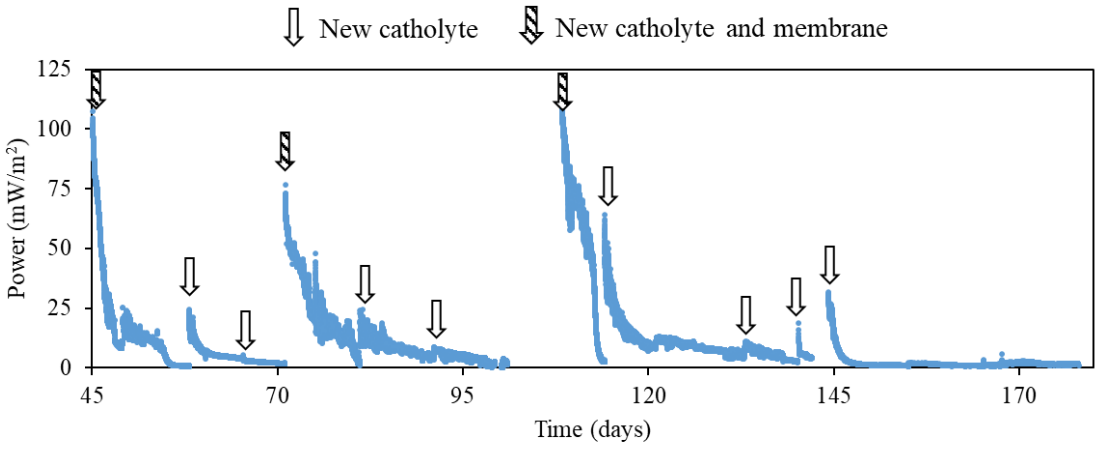

Fig. 3. Power generated from thermomechanical pulping wastewater in the up-flow MFC operated in continuous mode with a cation exchange membrane. The white arrow represents the replacement of catholyte with fresh ferricyanide solution, and the black-white arrow represents the replacement of both the membrane and catholyte.

As shown by the polarization data (Fig. 4) collected 10 days after CEM replacement on day 81, a maximum power of 28 mW/m^2 was obtained at a current density of 83 mA/m^2 (500 Ω external resistance). In the following days, the power production decreased, and a maximum power of only 15 mW/m^2 was obtained when the polarization analysis was repeated on day 94 (Fig. 3). This was attributed to the CEM fouling (see section 3.2.3), which caused an increase of the whole cell internal resistance from 470 Ω on day 81 to 786 Ω on day 94, as estimated from the slope of the linear part of the polarization curves (Fig. 4).

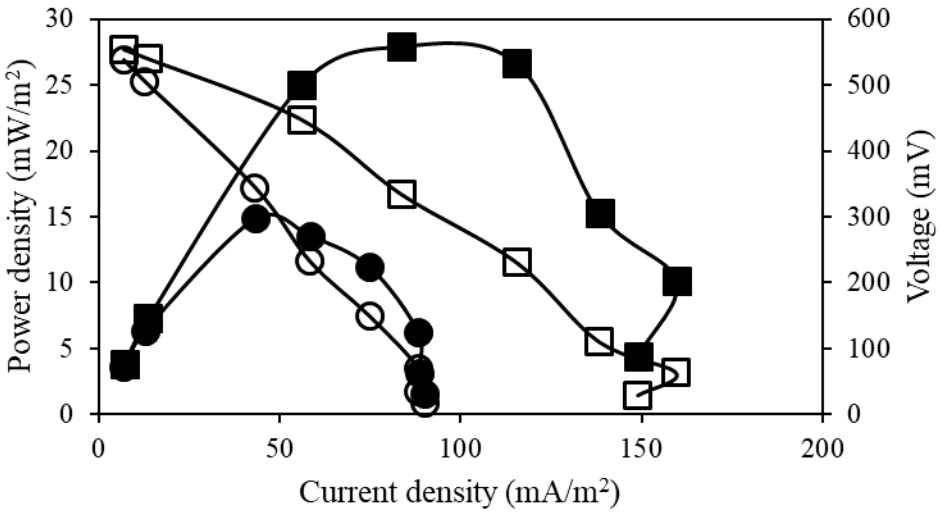

Fig. 4. Power (black) and polarization (white) curves obtained from the up-flow MFC continuously fed with thermomechanical pulping wastewater. The analysis was done with fresh (squares) and fouled (circles) cation exchange membrane on day 82 and 94, respectively.

A power density up to 71 mW/m^2 (during polarization) was obtained from wastewater produced by hydrothermal treatment of raw wood (3.3 g/L total COD) in an air-cathode MFC [14] as compared to 28 mW/m^2 obtained in this study. The characteristics of such wastewater were similar to those of the TMP wastewater used in this study, suggesting that the difference in power output can be attributed to the different MFC configuration. In particular, the distance between the anode and cathode electrode, in combination with the low conductivity of the TMP wastewater, likely resulted in high ohmic losses in this study.

3.2.2 COD removal from thermomechanical pulping wastewater

For continuous mode operation with TMP wastewater as the substrate (days 39-178), the up-flow MFC was fed with 4.1 (± 1.3) g/L total COD, of which 3.1 (± 0.5) g/L was soluble COD (Fig. 5).

The total COD concentration in the influent varied during the operation and increased occasionally up to 8-9 g/L (Fig. 5a) due to variations in the quantity of suspended solids in the feed (not removed by settling) or due to the detachment of biomass that colonized the influent tubes after the first two weeks of MFC operation with TMP wastewater. Microorganisms attached in the influent tubing were likely partially fermenting the sugars present in the TMP wastewater, resulting in a concentration of 0.7 (± 0.2) g/L COD acetate and 0.2 (± 0.1) g/L butyrate in the MFC influent, higher than the concentrations detected when characterizing the TMP wastewater (Table 1).

An average COD removal efficiency (both total and soluble) of 47-48% was obtained between days 45-178. This resulted in an effluent containing 2.1 (± 0.4) g/L total COD and 1.6 (± 0.3) g/L soluble COD (Fig. 5a and 5b), having a pH of 7.2 ± 0.3. This suggests that, despite the presence of recalcitrant compounds [3] and low concentration of nutrients (Table 1), TMP wastewater can be treated in an MFC to decrease its COD content. A lower total COD (29%) and a similar soluble COD removal (51%) efficiency was obtained by Huang and Logan [48] in a MFC treating paper recycling plant wastewater (1.4 and 0.2 g/L total and soluble COD). They were able to increase the total and soluble COD removal efficiencies to 70 and 75% upon addition of 50 mM phosphate buffer due to the increased conductivity and buffering capacity [48].

During continuous operation with TMP wastewater and AEM, the acetate concentration in the effluent increased up to 1.6 g/L COD on day 45, although the anolyte pH remained stable at 7 (± 0.2). When the AEM was replaced by a CEM, the acetate concentration in the effluent decreased to 0.4 g/L COD by day 70 (Fig. 5c), suggesting an increased activity of acetate utilizing

microorganisms although acetate was not totally consumed. This was likely due to the higher availability of protons for the cathodic reactions, and the consequent lower resistance for the electricity producing pathway at the anode. Butyrate and propionate were generally detected at low concentrations in the effluent, although butyrate reached 0.5 g/L COD on days 65-81, before decreasing again to < 0.1 g/L COD (Fig. 5c). On days 45-178, when the up-flow MFC was operated with a CEM, VFAs accounted for 44 (± 14) % of the soluble COD in the effluent, whereas monosaccharides were not detected. A share of the uncharacterized soluble COD was likely from derivates of lignin, which are recalcitrant to biological treatment and have been reported to account for 16-49% of COD in TMP wastewater [3].

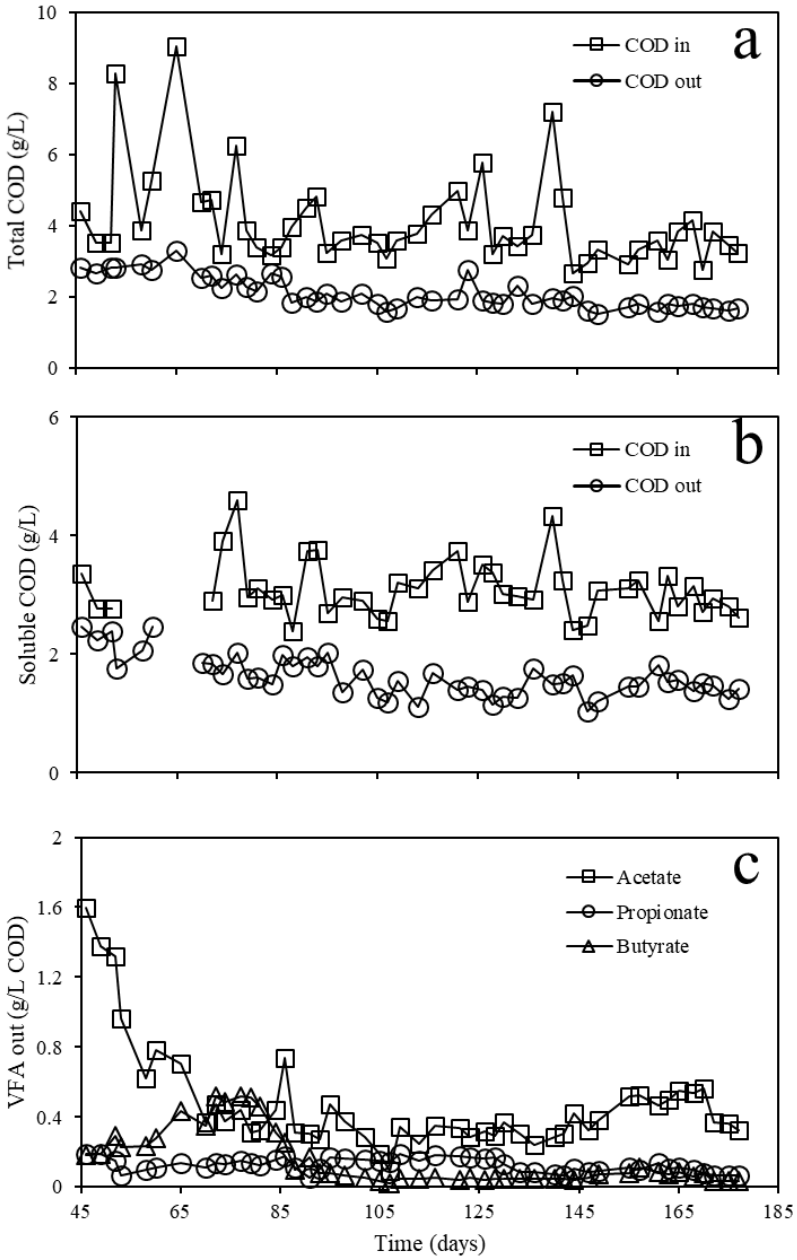

Fig. 5. Concentration of total (a) and soluble (b) COD in the influent and effluent of the up-flow MFC and volatile fatty acids detected in the effluent (c) during the operation in continuous mode with thermomehcanical pulping wastewater as the substrate using a cation exchange membrane.

3.2.3 Characterization of the membrane fouling

SEM-EDS analysis of the anodic side of the CEM after 30 days of operation showed a prevalence of inorganic fouling, which likely caused the power density drop from 70 mW/m^2 (on day 71) to 2 mW/m^2 (on day 101) (Fig. 3). Bacterial cells (Fig. 6 and S5) and nucleic acid (measured by Nanodrop) were not observed on the membrane surface in this study, confirming a minor role of biofouling. According to SEM-EDS, most of the surface of the membrane analysed was covered by crystals mainly consisting of calcium, phosphorous and oxygen (Fig. 6, S5a, S5b and S5c). Ca^{2+} ions, detected in the TMP wastewater with a concentration of 43.9 mg/L (Table 1), were likely occupying the active sites (sulphonate groups, Fig. S5d) of the CEM, as previously reported by Choi et al. [52]. The phosphorous concentration in the TMP wastewater was low (Table 1), but a cross-over of phosphate from the cathodic to the anodic chamber through the CEM cannot be excluded. However, such an issue is not relevant for possible full-scale application if the ferricyanide in phosphate buffer is replaced with a more sustainable catholyte such as air, or with a biocathode.

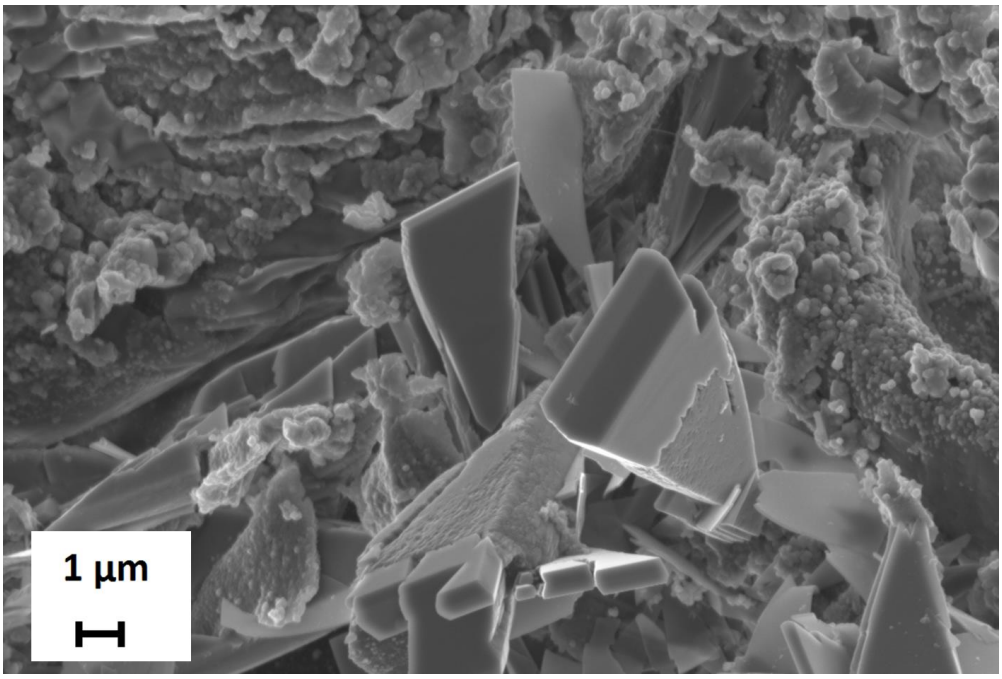

Fig. 6. SEM image of the crystalline structures found on the cation exchange membrane after 30 days of MFC operation with thermomechanical pulping wastewater containing 2 g/L $NaHCO_3$.

The EIS was performed to characterize the resistance of the CEMs used in the MFCs at different time points. As shown by the Nyquist plot of the EIS experimental data (Fig. 7a) and its simulation according to the equivalent circuit (Fig. 7b), the charge transfer resistance (R_{ct}) was the major kinetic limitation in the up-flow MFC. R_{ct} increased from 81 to 466 Ω, as estimated from the diameter of the semi-circles [53], due to CEM fouling, which limited proton conductivity. In fact, the internal resistance caused by the separator is a key factor in MFC performance [12], especially if the membrane has been fouled. As expected, the ohmic resistance (R_S), represented by the intercept of the impedance curves with the x-axis, was about 95-100 Ω regardless of the fouling level of the CEM.

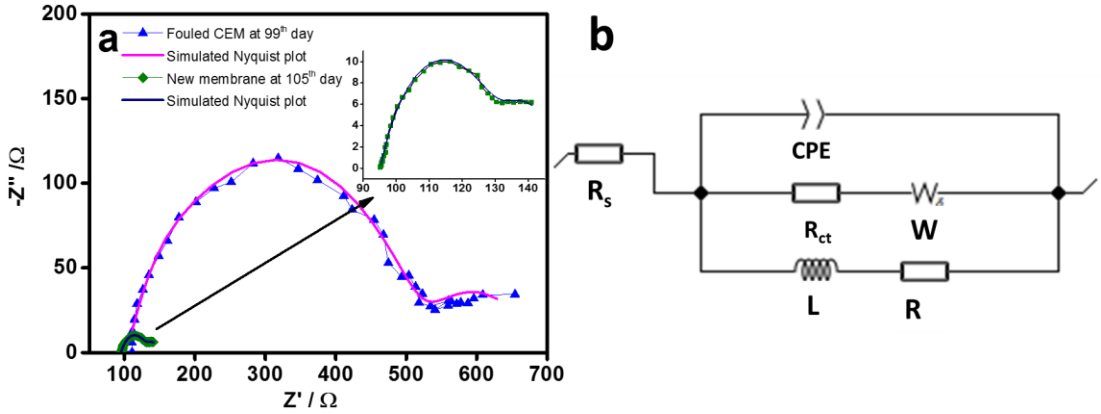

Fig. 7. Nyquist plot of the impedance spectrum obtained from the up-flow MFC continuously fed with thermomechanical pulping wastewater with fresh and fouled cation exchange membrane (a) and best fit circuit diagram for the up-flow MFC used in this study (b).

3.3 Practical implications

The results of this study suggest that bioelectrochemical pretreatment can be implemented to reduce the COD concentration of TMP wastewater by about 50%. This would reduce the energy required for aeration in the subsequent conventional activated sludge process, which is typically 900-1000 Wh/kg COD removed [54], as well as generate an average electrical power of 3.5-5 Wh/kg COD removed (10-15 mW/m^2) with a 1.8 days HRT. However, for further process development, ferricyanide should be replaced with an air cathode or biocathode to reduce costs and environmental impacts, and distance between anode and cathode electrodes should be reduced to improve the power production and CE by decreasing internal resistance.

Sustainability of the electrode materials could be enhanced by replacing the GAC with e.g. conductive biochar granules obtained from high temperature pyrolysis of waste material. For example, the use of biochar from coconut shells as anode in sediment MFCs has been reported

by Chen et al. [56]. Alternatively, the GAC granules could be fluidized to decrease mass transport limitations [23].

In case of fouling, mitigation strategies such as modification of membrane charge, hydrophobicity and roughness, use of cleaning agents, and electrical methods such as polarity reversal, pulse electric field or overlimiting current regime need to be evaluated [55]. Among them, a pulse electric field can be easily implemented to MFCs using a square electric wave generator connected to the two electrodes. The application of 8 mA/cm^2 (10 V) pulses for 2 h, with a sequence of 2.5 s pulse and 0.5 s pause were tested during this study, but they failed in remediating the fouled CEM (50 days MFC operation with TMP wastewater, results not shown). Higher voltages and optimized sequence time could possibly help in reducing membrane fouling, but installation of an auxiliary anode electrode is suggested for applying the pulses to avoid damaging the anodic microbial community [56].

4. Conclusions

Similar power output and theoretical COD removals are obtained from xylose during stable operation of an up-flow MFC with graphite plate, carbon cloth and granular activated carbon in stainless steel cage anode electrodes. Carbon cloth enables the highest power density (333 mW/m^2). However, granular activated carbon in stainless steel cage is considered the most suitable anode electrode for bioelectrochemical treatment based on its high current density in a wide potential range, high surface area and scalability.

Long-term continuous operation with TMP wastewater results in 47% total COD removal with an average power output of 10-15 mW/m^2 at an HRT of 1.8 d. To our knowledge, this is the first report on bioelectrochemical treatment of TMP wastewater. Bioelectrochemical pretreatment reduces the COD load of TMP wastewater, decreasing the energy required for aeration in the aerobic treatment whilst the Coulombic efficiency remains low.

Acknowledgements

This work was supported by the Academy of Finland (New Indigo ERA-Net Energy 2014; Project no. 283013) and the Marie Skłodowska-Curie European Joint Doctorate (EJD) in Advanced Biological Waste-To-Energy Technologies (ABWET) funded from Horizon 2020 under grant agreement no. 643071. This work utilized the Tampere Microscopy Center facilities at Tampere University (Finland).

Conflict of interest

The authors declare no conflict of interest.

References

[1] T. Meyer, E.A. Edwards, Anaerobic digestion of pulp and paper mill wastewater and sludge, Water Res. 65 (2014) 321–349.

[2] M. Kamali, Z. Khodaparast, Review on recent developments on pulp and paper mill wastewater treatment, Ecotoxicol. Environ. Saf. 114 (2015) 326–342.

[3] J.A. Rintala, J.A. Puhakka, Anaerobic treatment in pulp- and paper-mill waste management: A review, Bioresour. Technol. 47 (1994) 1–18.

[4] W.J. Gao, M.N. Han, C.C. Xu, B.Q. Liao, Y. Hong, J. Cumin, M. Dagnew, Performance of submerged anaerobic membrane bioreactor for thermomechanical pulping wastewater treatment, J. Water Process Eng. 13 (2016) 70–78.

[5] J.A. Rintala, S.S. Lepistö, Anaerobic treatment of thermomechanical pulping whitewater at 35-70°C, Water Res. 26 (1992) 1297–1305.

[6] P. Dessì, E. Porca, A.M. Lakaniemi, G. Collins, P.N.L. Lens, Temperature control as key factor for optimal biohydrogen production from thermomechanical pulping wastewater, Biochem. Eng. J. 137 (2018) 214–221.

[7] S.K. Butti, G. Velvizhi, M.L.K. Sulonen, J.M. Haavisto, E. Oguz Koroglu, A. Yusuf Cetinkaya, S. Singh, D. Arya, J. Annie Modestra, K. Vamsi Krishna, A. Verma, B. Ozkaya, A.-M. Lakaniemi, J.A. Puhakka, S. Venkata Mohan, Microbial electrochemical technologies with the perspective of harnessing bioenergy: Maneuvering towards upscaling, Renew. Sustain. Energy Rev. 53 (2016) 462–476.

[8] B.E. Logan, K. Rabaey, Conversion of wastes into bioelectricity and chemicals by using microbial electrochemical technologies, Science. 337 (2012) 686–690.

[9] B.E. Logan, B. Hamelers, R. Rozendal, U. Schröder, J. Keller, S. Freguia, P. Aelterman, W. Verstraete, K. Rabaey, Microbial fuel cells: Methodology and technology, Environ. Sci. Technol. 40 (2006) 5181–5192.

[10] P. Liang, R. Duan, Y. Jiang, X. Zhang, Y. Qiu, X. Huang, One-year operation of 1000-L modularized microbial fuel cell for municipal wastewater treatment, Water Res. 141 (2018) 1–8.

[11] J. Choi, Y. Ahn, Continuous electricity generation in stacked air cathode microbial fuel cell treating domestic wastewater, J. Environ. Manage. 130 (2013) 146–152.

[12] B. Min, J.R. Kim, S.E. Oh, J.M. Regan, B.E. Logan, Electricity generation from swine wastewater using microbial fuel cells, Water Res. 39 (2005) 4961–4968.

[13] A. Callegari, D. Cecconet, D. Molognoni, A.G. Capodaglio, Sustainable processing of dairy wastewater: Long-term pilot application of a bio-electrochemical system, J. Clean. Prod. 189 (2018) 563–569.

[14] R. Toczyłowska-Mamińska, K. Szymona, M. Kloch, Bioelectricity production from wood hydrothermal-treatment wastewater: Enhanced power generation in MFC-fed mixed wastewaters, Sci. Total Environ. 634 (2018) 586–594.

[15] U. Abbasi, W. Jin, A. Pervez, A.Z. Bhatti, M. Tariq, S. Shaheen, A. Iqbal, Q. Mahmood, Anaerobic microbial fuel cell treating combined industrial wastewater: Correlation of electricity generation with pollutants, Bioresour. Technol. 200 (2016) 1–7.

[16] C. Feng, Z. Lv, X. Yang, C. Wei, Anode modification with capacitive materials for a microbial fuel cell: An increase in transient power or stationary power, Phys. Chem. Chem. Phys. 16 (2014) 10464–10472.

[17] C. Santoro, C. Arbizzani, B. Erable, I. Ieropoulos, Microbial fuel cells: From fundamentals to applications. A review, J. Power Sources. 356 (2017) 225–244.

[18] K. Guo, D. Hidalgo, T. Tommasi, K. Rabaey, Pyrolytic carbon-coated stainless steel felt as a high-performance anode for bioelectrochemical systems, Bioresour. Technol. 211 (2016) 664–668.

[19] J. Hou, Z. Liu, Y. Li, S. Yang, Y. Zhou, A comparative study of graphene-coated stainless steel fiber felt and carbon cloth as anodes in MFCs, Bioprocess Biosyst. Eng. 38 (2015) 881–888.

[20] S. Cheng, B.E. Logan, Ammonia treatment of carbon cloth anodes to enhance power

generation of microbial fuel cells, Electrochem. Commun. 9 (2007) 492–496.

[21] X. Wang, S. Cheng, Y. Feng, M.D. Merrill, T. Saito, B.E. Logan, Use of carbon mesh anodes and the effect of different pretreatment methods on power production in microbial fuel cells, Environ. Sci. Technol. 43 (2009) 6870–6874.

[22] X.-Y. Wu, F. Tong, T.-S. Song, X.-Y. Gao, J.-J. Xie, C.C. Zhou, L.-X. Zhang, P. Wei, Effect of zeolite-coated anode on the performance of microbial fuel cells, J. Chem. Technol. Biotechnol. 90 (2015) 87–92.

[23] J. Liu, F. Zhang, W. He, X. Zhang, Y. Feng, B.E. Logan, Intermittent contact of fluidized anode particles containing exoelectrogenic biofilms for continuous power generation in microbial fuel cells, J. Power Sources. 261 (2014) 278–284.

[24] A. Deeke, T.H.J.A. Sleutels, T.F.W. Donkers, H.V.M. Hamelers, C.J.N. Buisman, A. Ter Heijne, Fluidized capacitive bioanode as a novel reactor concept for the microbial fuel cell, Environ. Sci. Technol. 49 (2015) 1929–1935.

[25] K.R. Fradler, J.R. Kim, H.C. Boghani, R.M. Dinsdale, A.J. Guwy, G.C. Premier, The effect of internal capacitance on power quality and energy efficiency in a tubular microbial fuel cell, Process Biochem. 49 (2014) 973–980.

[26] J.M. Haavisto, A.M. Lakaniemi, J.A. Puhakka, Storing of exoelectrogenic anolyte for efficient microbial fuel cell recovery, Environ. Technol. 17 (2018) 1–9.

[27] A.E. Mäkinen, M.E. Nissilä, J.A. Puhakka, Dark fermentative hydrogen production from xylose by a hot spring enrichment culture, Int. J. Hydrogen Energy. 37 (2012) 12234–12240.

[28] K.J. Balkus, K.T. Ly, The preparation and characterization of an X-type zeolite: An experiment in solid-state chemistry, J. Chem. Educ. 68 (1991) 875–877.

[29] X. Wu, F. Tong, X. Yong, J. Zhou, L. Zhang, H. Jia, Effect of NaX zeolite-modified graphite felts on hexavalent chromium removal in biocathode microbial fuel cells, J. Hazard. Mater. 308 (2016) 303–311.

[30] C.H. Lay, M.E. Kokko, J.A. Puhakka, Power generation in fed-batch and continuous up-flow microbial fuel cell from synthetic wastewater, Energy. 91 (2015) 235–241.

[31] APHA, Standard Methods for the Examination of Water and Wastewater, twentieth ed. American Public Health Association/American Water Works Association/Water Environment Federation, Washington DC., (1998).

[32] M. Dubois, K. Gilles, J.K. Hamilton, P. Rebers, F. Smith, Colorimetric method for determination of sugars and related substances, Anal. Chem. 28 (1956) 350–356.

[33] J.M. Haavisto, M.E. Kokko, C.-H. Lay, J.A. Puhakka, Effect of hydraulic retention time on continuous electricity production from xylose in up-flow microbial fuel cell, Int. J. Hydrogen Energy. 42 (2017) 27494–27501.

[34] P. Dessì, E. Porca, J. Haavisto, A.-M. Lakaniemi, G. Collins, P.N.L. Lens, Composition and role of the attached and planktonic active microbial communities in mesophilic and thermophilic xylose-fed microbial fuel cells, RSC Adv. 8 (2018) 3069–3080.

[35] A. Van Haandel, J. Van der Lubbe, Handbook of biological wastewater treatment: Design and Optimisation of Activated Sludge Systems, Quist Publishing, Leidschendam, The Netherlands, 2012.

[36] X. Zhu, B.E. Logan, Copper anode corrosion affects power generation in microbial fuel cells, J. Chem. Technol. Biotechnol. 89 (2014) 471–474.

[37] E. Taskan, H. Hasar, Comprehensive comparison of a new tin-coated copper mesh and a graphite plate electrode as an anode material in microbial fuel cell, Appl. Biochem.

Biotechnol. 175 (2014) 2300–2308.

[38] D. Pocaznoi, A. Calmet, L. Etcheverry, B. Erable, A. Bergel, Stainless steel is a promising electrode material for anodes of microbial fuel cells, Energy Environ. Sci. 5 (2012) 9645–9652.

[39] J. Liu, F. Zhang, W. He, W. Yang, Y. Feng, B.E. Logan, A microbial fluidized electrode electrolysis cell (MFEEC) for enhanced hydrogen production, J. Power Sources. 271 (2014) 530–533.

[40] J.N. Roy, S. Babanova, K.E. Garcia, J. Cornejo, L.K. Ista, P. Atanassov, Catalytic biofilm formation by *Shewanella oneidensis* MR-1 and anode characterization by expanded uncertainty, Electrochim. Acta. 126 (2014) 3–10.

[41] X. Zhu, J.C. Tokash, Y. Hong, B.E. Logan, Controlling the occurrence of power overshoot by adapting microbial fuel cells to high anode potentials, Bioelectrochemistry. 90 (2013) 30–35.

[42] C.I. Torres, A.K. Marcus, B.E. Rittmann, Proton transport inside the biofilm limits electrical current generation by anode-respiring bacteria, Biotechnol. Bioeng. 100 (2008) 872–881.

[43] H.S. Lee, P. Parameswaran, A. Kato-Marcus, C.I. Torres, B.E. Rittmann, Evaluation of energy-conversion efficiencies in microbial fuel cells (MFCs) utilizing fermentable and non-fermentable substrates, Water Res. 42 (2008) 1501–1510.

[44] X.L. Zhou, T.S. Zhao, Y.K. Zeng, L. An, L. Wei, A highly permeable and enhanced surface area carbon-cloth electrode for vanadium redox flow batteries, J. Power Sources. 329 (2016) 247–254.

[45] A. ter Heijne, H.V.M. Hamelers, M. Saakes, C.J.N. Buisman, Performance of non-porous

graphite and titanium-based anodes in microbial fuel cells, Electrochim. Acta. 53 (2008) 5697–5703.

[46] D. Mohan, K. Singh, Granular activated carbon, Water encyclopedia (eds. J. H. Lehr and J. Keeley), 2005.

[47] M. Miskan, M. Ismail, M. Ghasemi, J. Md Jahim, D. Nordin, M.H. Abu Bakar, Characterization of membrane biofouling and its effect on the performance of microbial fuel cell, Int. J. Hydrogen Energy. 41 (2016) 543–552.

[48] L. Huang, B.E. Logan, Electricity generation and treatment of paper recycling wastewater using a microbial fuel cell, Appl. Microbiol. Biotechnol. 80 (2008) 349–355.

[49] Y. Yuan, B. Zhao, S. Zhou, S. Zhong, L. Zhuang, Electrocatalytic activity of anodic biofilm responses to pH changes in microbial fuel cells, Bioresour. Technol. 102 (2011) 6887–6891.

[50] J.R. Kim, S. Cheng, S.-E. Oh, B.E. Logan, Power generation using different cation, anion, and ultrafiltration membranes in microbial fuel cells, Environ. Sci. Technol. 41 (2007) 1004–1009.

[51] S. Freguia, K. Rabaey, Z. Yuan, J. Keller, Electron and carbon balances in microbial fuel cells reveal temporary bacterial storage behavior during electricity generation, Environ. Sci. Technol. 41 (2007) 2915–2921.

[52] M.-J. Choi, K.-J. Chae, F.F. Ajayi, K.-Y. Kim, H.-W. Yu, C. Kim, I.S. Kim, Effects of biofouling on ion transport through cation exchange membranes and microbial fuel cell performance, Bioresour. Technol. 102 (2011) 298–303.

[53] M.T. Noori, S.C. Jain, M.M. Ghangrekar, C.K. Mukherjee, Biofouling inhibition and enhancing performance of microbial fuel cell using silver nano-particles as fungicide and

cathode catalyst, Bioresour. Technol. 220 (2016) 183–189.

[54] G. Mininni, G. Laera, G. Bertanza, M. Canato, A. Sbrilli, Mass and energy balances of sludge processing in reference and upgraded wastewater treatment plants, Environ. Sci. Pollut. Res. 22 (2015) 7203–7215.

[55] S. Mikhaylin, L. Bazinet, Fouling on ion-exchange membranes: Classification, characterization and strategies of prevention and control, Adv. Colloid Interface Sci. 229 (2016) 34–56.

[56] S.E. Oh, J.R. Kim, J.H. Joo, B.E. Logan, Effects of applied voltages and dissolved oxygen on sustained power generation by microbial fuel cells, Water Sci. Technol. 60 (2009) 1311–1317.

Effects of anode materials on electricity production from xylose and treatability of TMP wastewater in an up-flow microbial fuel cell

Johanna Haavisto [a,#], Paolo Dessì [a, b, #,], Pritha Chatterjee [a,c], Mari Honkanen [d], Md Tabish Noori [e], Marika Kokko [a], Aino-Maija Lakaniemi [a], Piet N. L. Lens [a, b], Jaakko A. Puhakka [a]*

SUPPORTING INFORMATION

[a]*Tampere University, Faculty of Engineering and Natural Sciences, PO Box 541, FI-33104 Tampere University, Finland*

[b]*National University of Ireland Galway, Microbiology, School of Natural Sciences and Ryan Institute, University Road, Galway, H91 TK33, Ireland*

[c]*Indian Institute of Technology Hyderabad, Department of Civil Engineering, Hyderabad, India*

[d]*Tampere University, Tampere Microscopy Center, PO Box 692, FI-33104 Tampere University, Finland*

[e]*Kyung Hee University, Department of Environmental Science and Engineering, 446701, Seoul, South Korea*

*****Corresponding author: Phone: +353 830678774, e-mail: paolo.dessi@nuigalway.ie, mail: National University of Ireland Galway, Microbiology, School of Natural Sciences and Ryan Institute, University Road, Galway, H91 TK33, Ireland

[#] These two authors contributed equally to the manuscript

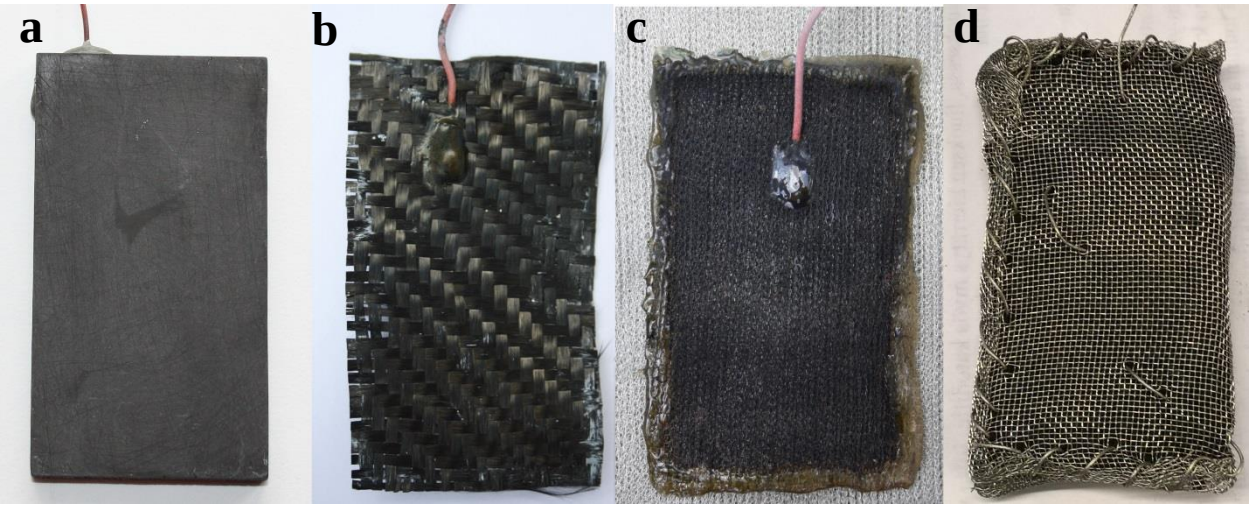

Figure S1. Photos of a) graphite plate, b) carbon cloth with zeolite coating and c) tin coated copper mesh after use, and d) granular activated carbon in stainless steel cage before use. The appearance of the graphite plate and carbon cloths (bare and zeolite coated) did not change during the MFC operation. The tin coated copper mesh electrode is placed over a similar unused mesh to show a clear color difference caused by copper oxidation. Copper wires were used as current collectors with all the other materials, but stainless steel cage was closed with titanium wire and the end of the wire was also used as current collector.

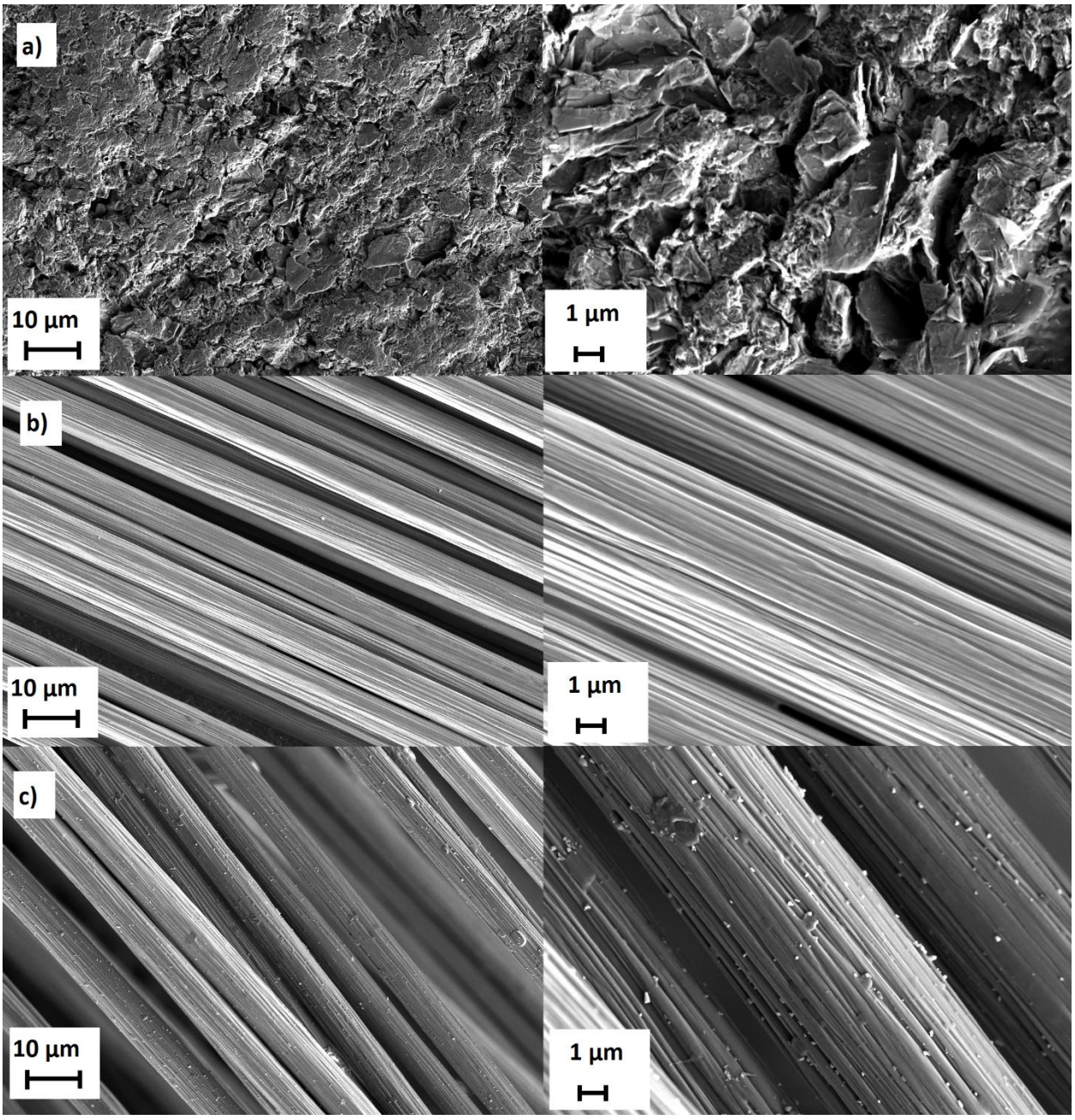
a)
10 µm
1 µm
b)
10 µm
1 µm
c)
10 µm
1 µm

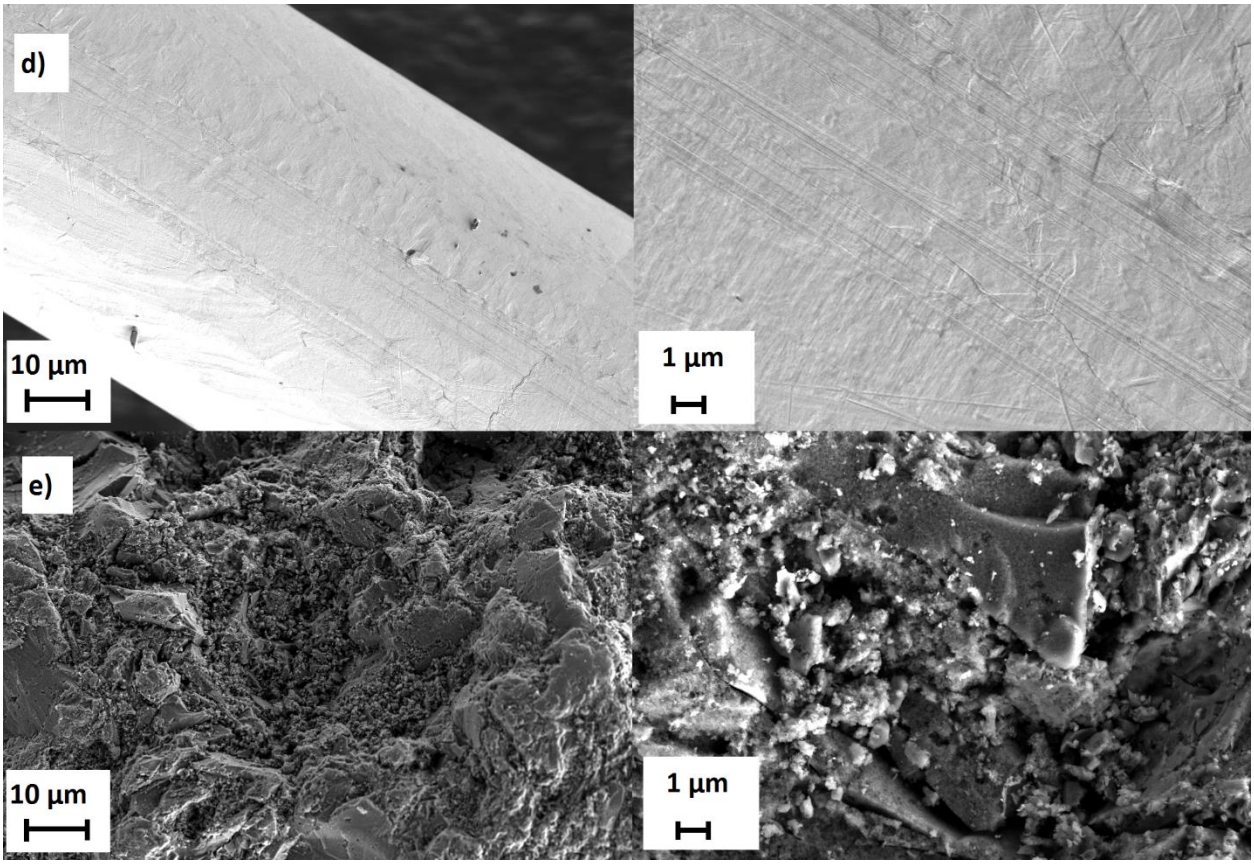

Figure S2. SEM images of the clean electrode materials with two different magnifications for each material. Graphite plate (a), carbon cloth (b), zeolite coated carbon cloth (c), tin coated copper (d), and granular activated carbon (e).

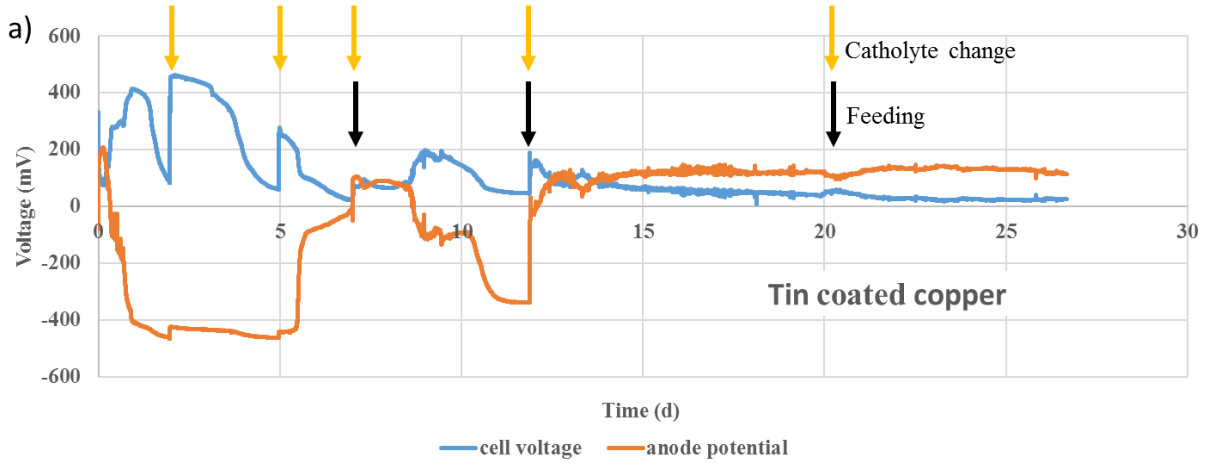
a)
Catholyte change
Feeding
Tin coated copper
Voltage (mV)
Time (d)
cell voltage
anode potential

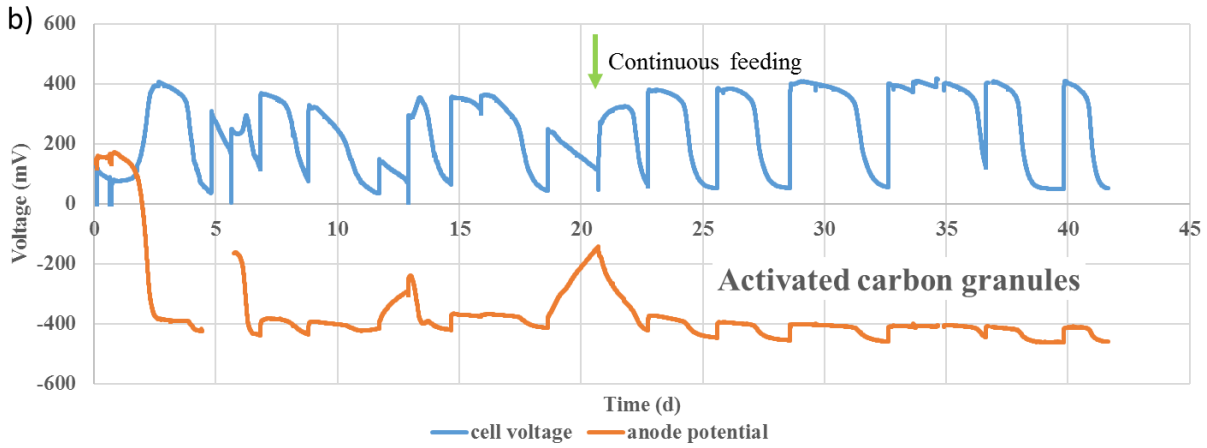
b)
Continuous feeding
Activated carbon granules
Voltage (mV)
Time (d)
cell voltage
anode potential

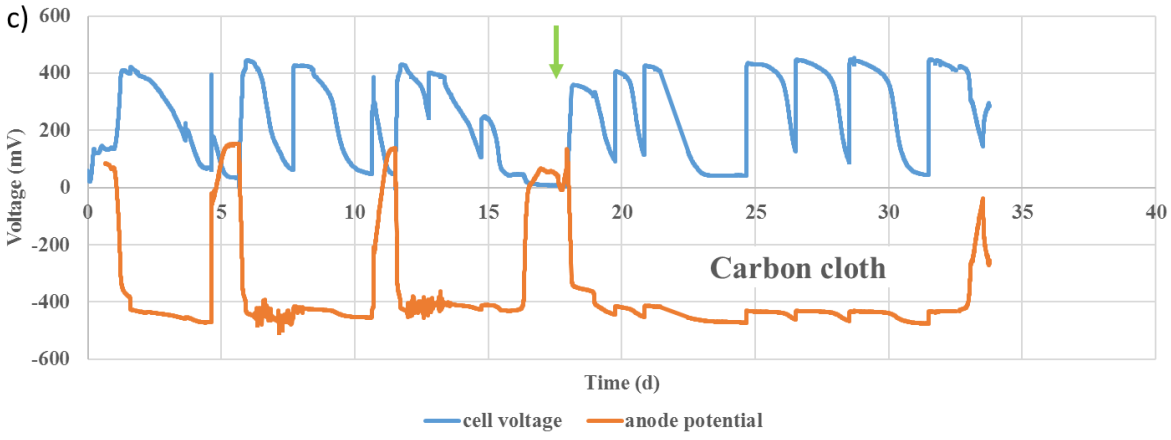
c)
Carbon cloth
Voltage (mV)
Time (d)
cell voltage
anode potential

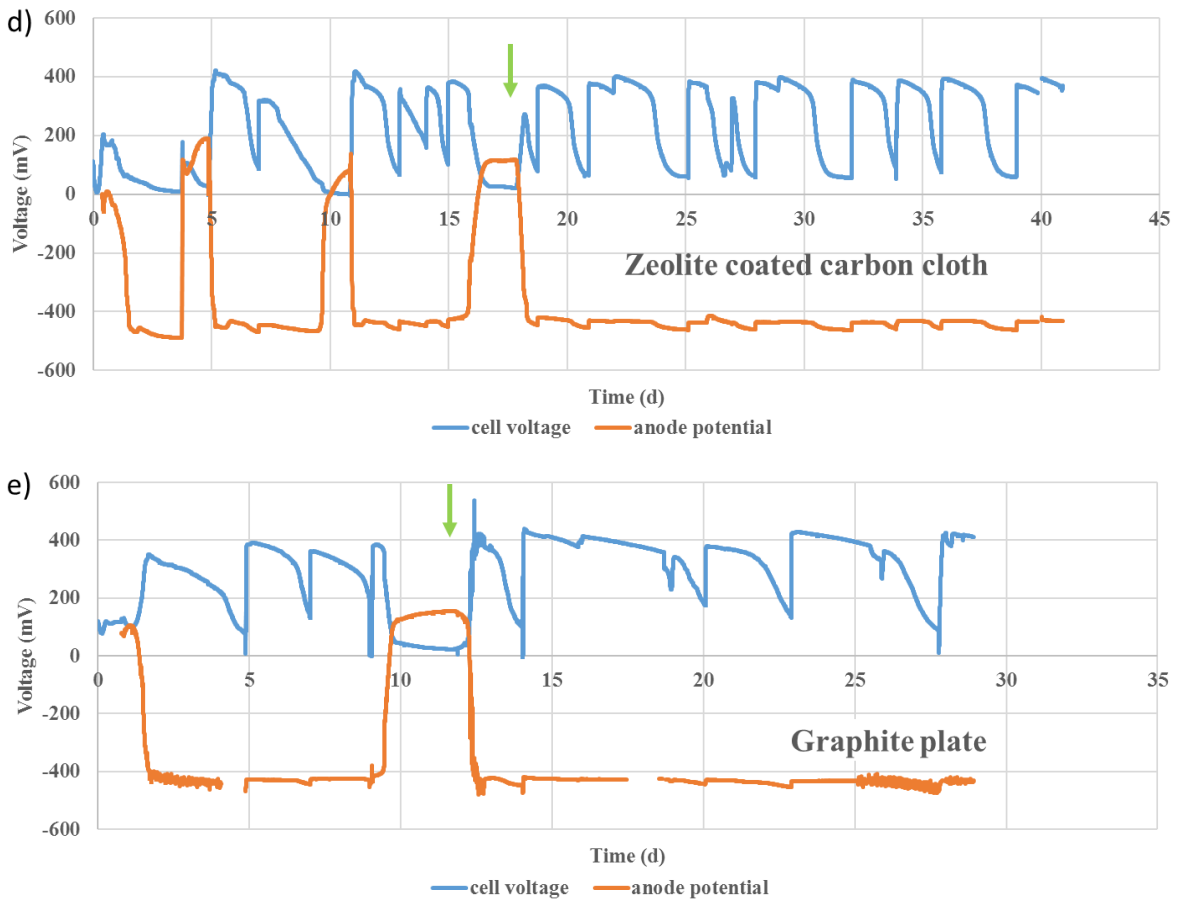

Figure S3. Cell voltages and anode potentials as a function of time with the different anode electrodes. The effect of feeding (black arrows) and catholyte changes (yellow arrows) are shown for a) tin coated copper as an example. For b) activated carbon granules, c) carbon cloth, d) zeolite coated carbon cloth, and e) graphite plate the green arrows show the starting point of continuous feeding.

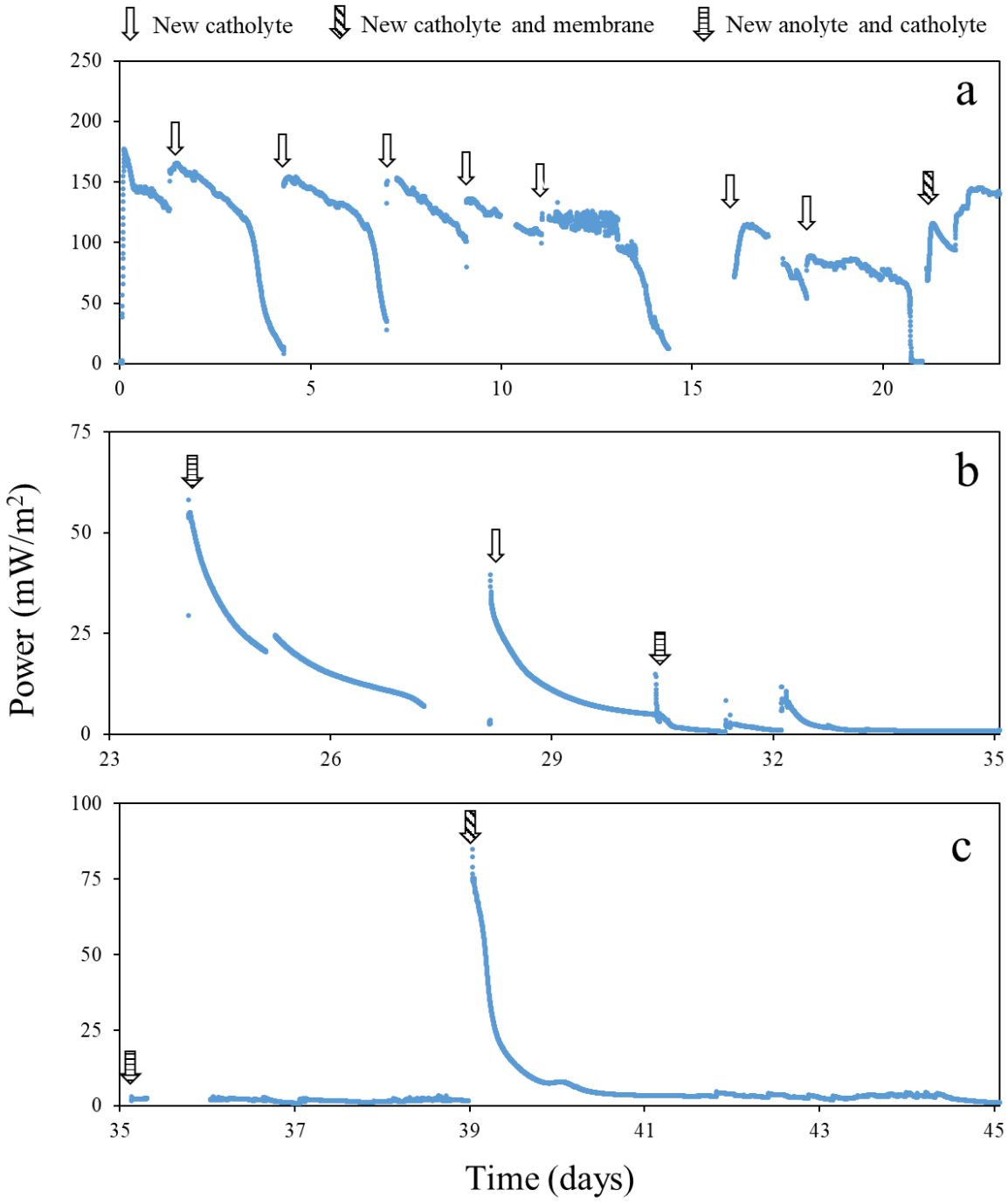

Figure S4. Power generated from thermomechanical pulping wastewater in the upflow MFC operated with an AEM and fed in continuous mode with xylose (a), and in semi-continuous (b) or continuous (c) mode with TMP wastewater.

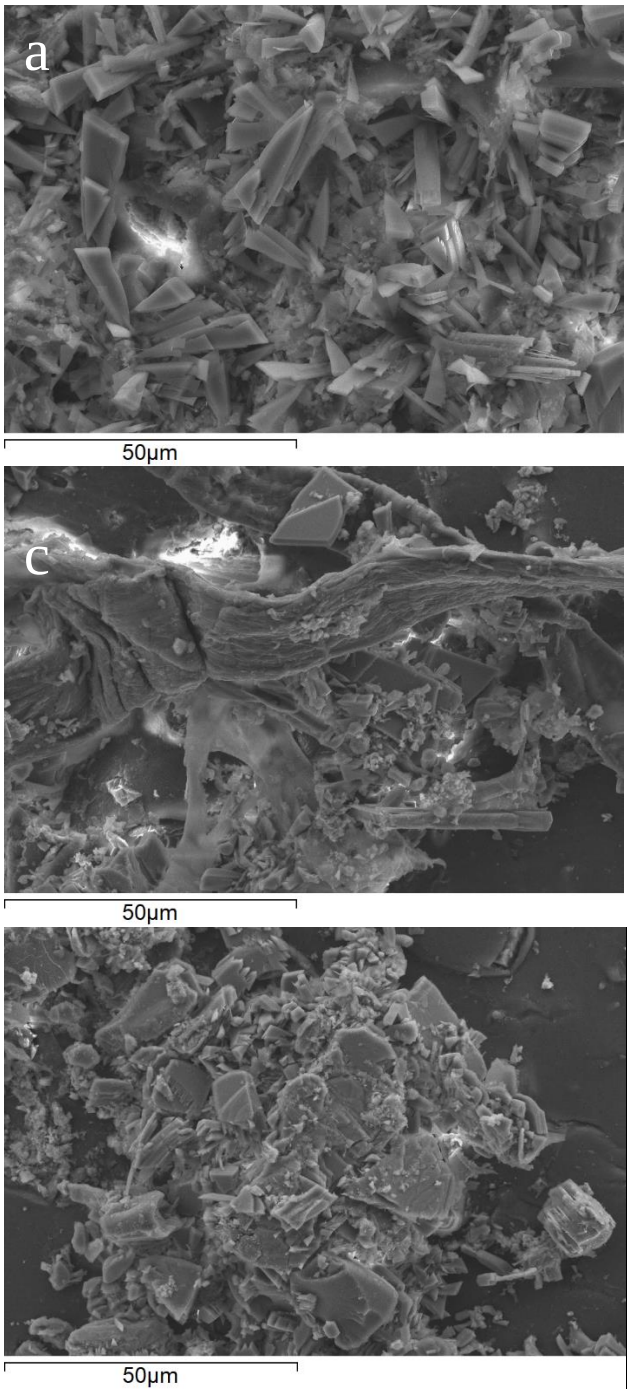
a
50µm
c
50µm
50µm

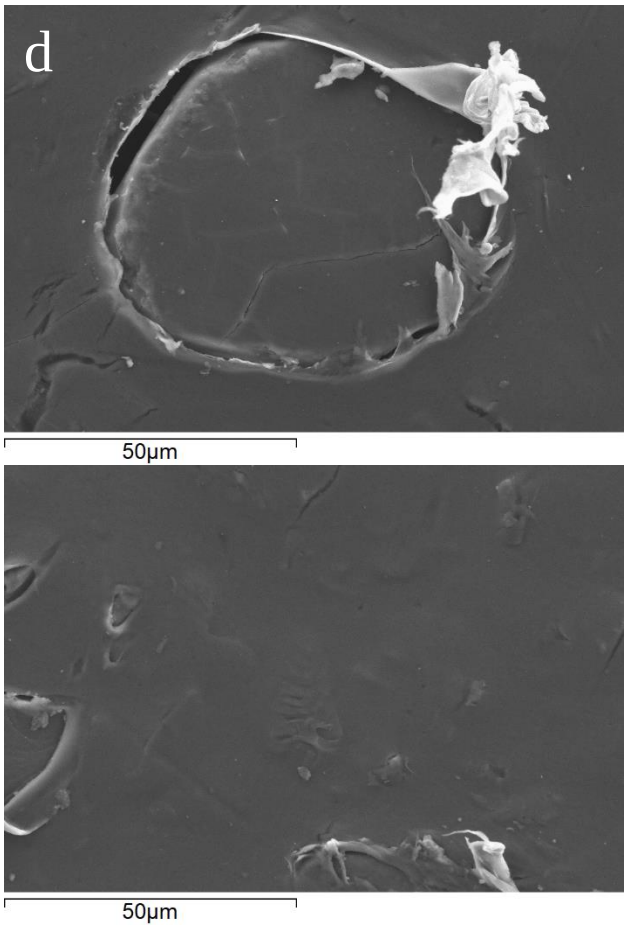

Figure S5. SEM images of three different points of the fouled CEM after approximately 30 days of continuous up-flow MFC operation with thermomechanical pulping wastewater (a, b, c), as well as the active site (d) and frame (e) of the fresh CEM.

Table S1. Criteria for electrode scalability, which were chosen to evaluate the potential of the anode electrodes for full-scale operation. Short distances between anode and cathode electrodes and high electrode conductivity are required to decrease the internal resistances and good chemical and mechanical strength are required to keep large electrodes intact during long-term operation.

Anode electrode	**Potential for using electrode material in different reactor**	**Conductivity[a]**	**Chemical and mechanical strength**	**Overall evaluation[b]**

	configurations			
Carbon cloth	Thin, flexible material that has been used in various MFC configurations [1–4]	++	Low mechanical strength due to loose weaving. Corrosion resistant [5]	++
Graphite plate	Thick, hard material that can be used as flat plate [6,7]	+++	Relatively high mechanical strength although brittle [8] Corrosion resistant [5]	++
GAC in SS cage	Adaptable to various electrode and MFC configurations [9–11]. 3D structure that can also be fluidized [12].	++ for GAC +++ for SS	High mechanical strength due to the stainless steel cage. GAC: corrosion resistant [5] SS: corrosion resistant as MFC anode under anaerobic conditions [13]	+++
Zeolite coated carbon cloth	Thin, flexible material that can be used in various MFC configurations in a similar way to carbon cloth	++	Low mechanical strength due to loose weaving. Corrosion resistant [5]	++
Tin coated copper	Thin, flexible material that has been studied in simple MFC configurations [14,15]	+++	The material was oxidized in only 3 days in this study	+

[a] Anode material conductivities: carbon cloth 333 S/m [16]; graphite plate 3×10^5 S/m [17]; GAC 748 S/m [16], stainless steel and copper $>1x10^6$ S/m [17]. The lower conductivity of GAC compared to graphite plate can be compensated with close contact to SS cage or by frequent collisions to SS in fluidized bed; (>1000 S/m +++, 100-1000 S/m ++, < 100 S/m +)

[b] Overall evaluation is based on the flexibility, conductivity and chemical and mechanical strength of the electrode (all aspects satisfactory +++, at least one aspect challenging ++, at least one aspect failing +)

References

[1] S. Hays, F. Zhang, B.E. Logan, Performance of two different types of anodes in membrane electrode assembly microbial fuel cells for power generation from domestic wastewater, J. Power Sources. 196 (2011) 8293–8300.

[2] H. Yazdi, L. Alzate-Gaviria, Z.J. Ren, Pluggable microbial fuel cell stacks for septic wastewater treatment and electricity production, Bioresour. Technol. 180 (2015) 258–263. doi:10.1016/j.biortech.2014.12.100.

[3] H. Liu, S. Cheng, L. Huang, B.E. Logan, Scale-up of membrane-free single-chamber microbial fuel cells, J. Power Sources. 179 (2008) 274–279.

[4] S.-H. Chang, B.-Y. Huang, T.-H. Wan, J.-Z. Chen, B.-Y. Chen, Surface modification of carbon cloth anodes for microbial fuel cells using atmospheric-pressure plasma jet processed reduced graphene oxides, RSC Adv. 7 (2017) 56433–56439.

[5] C. Santoro, C. Arbizzani, B. Erable, I. Ieropoulos, Microbial fuel cells: From

fundamentals to applications. A review, J. Power Sources. 356 (2017) 225–244.

[6] J.M. Haavisto, M.E. Kokko, C.-H. Lay, J.A. Puhakka, Effect of hydraulic retention time on continuous electricity production from xylose in up-flow microbial fuel cell, Int. J. Hydrogen Energy. 42 (2017) 27494–27501.

[7] A. Dewan, H. Beyenal, Z. Lewandowski, Scaling up microbial fuel cells, Environ. Sci. Technol. 42 (2008) 7643–7648.

[8] L.G. Borzani Manhani, L.C. Pardini, F.L. Neto, Assessement of tensile strength of graphites by the Iosipescu Coupon test, Mater. Res. 10 (2007) 233–239.

[9] D. Jiang, B. Li, Granular activated carbon single-chamber microbial fuel cells (GAC-SCMFCs): A design suitable for large-scale wastewater treatment processes, Biochem. Eng. J. 47 (2009) 31–37.

[10] S. Wu, H. Li, X. Zhou, P. Liang, X. Zhang, Y. Jiang, X. Huang, A novel pilot-scale stacked microbial fuel cell for efficient electricity generation and wastewater treatment, Water Res. 98 (2016) 396–403.

[11] D. Jiang, M. Curtis, E. Troop, K. Scheible, J. McGrath, B. Hu, S. Suib, D. Raymond, B. Li, A pilot-scale study on utilizing multi-anode/cathode microbial fuel cells (MAC MFCs) to enhance the power production in wastewater treatment, Int. J. Hydrogen Energy. 36 (2011) 876–884.

[12] A. Deeke, T.H.J.A. Sleutels, T.F.W. Donkers, H.V.M. Hamelers, C.J.N. Buisman, A. Ter Heijne, Fluidized capacitive bioanode as a novel reactor concept for the microbial fuel cell, Environ. Sci. Technol. 49 (2015) 1929–1935.

[13] E. Guerrini, P. Cristiani, M. Grattieri, C. Santoro, B. Li, S. Trasatti, Electrochemical behavior of stainless steel anodes in membraneless microbial fuel cells, J. Electrochem. Soc. 161 (2014) H62–H67.

[14] E. Taskan, H. Hasar, Comprehensive comparison of a new tin-coated copper mesh and a graphite plate electrode as an anode material in microbial fuel cell, Appl. Biochem. Biotechnol. 175 (2014) 2300–2308.

[15] E. Taskan, B. Ozkaya, H. Hasar, Comprehensive evaluation of two different inoculums in MFC with a new tin-coated copper mesh anode electrode for producing electricity from a cottonseed oil industry effluent, Environ. Prog. Sustain. Energy. 35 (2016) 110–116.

[16] U. Karra, S.S. Manickam, J.R. McCutcheon, N. Patel, B. Li, Power generation and organics removal from wastewater using activated carbon nanofiber (ACNF) microbial fuel cells (MFCs), Int. J. Hydrogen Energy. 38 (2013) 1588–1597.

[17] M. Helmenstine, Table of Electrical Resistivity and Conductivity, Https://Www.Thoughtco.Com/Table-of-Electrical-Resistivity-Conductivity-608499. (2019) 1–4.